Universidad Zaragoza
1542

Trabajo Fin de Máster

Evaluation of the performance of optimizer based PV systems under shading conditions

Autora

Virginia Cebollada Alvarez

Director/es

Björn O Karlsson
Nicholas Etherden

Escuela de Ingeniería y Arquitectura

2019

Abstract

Total or partial shading conditions have a detrimental impact in the output energy of photovoltaic (PV) systems and in the semiconductor materials PV technologies are made of. Residential PV installations are very likely to be exposed to shade projected by nearby objects such as buildings or neighboring trees. The electrical configuration of PV systems is crucial to mitigate the shading effect, as it is the use of power optimizers. This study assesses the shading impact on two different types of residential PV systems to verify gains associated with SolarEdge optimizers and support product marketing. It aspires to help PV owners select power inverters that maximize the annual energy produced. Experiments have been performed simulating snow coverage and tree shading on a string-based system (Fronius) and an optimizer-based system (SolarEdge). Findings demonstrated the decrease in losses from partial shading conditions with power optimizers. SolarEdge optimizers reduce shading power losses from 50% to 29% in comparison to a standard string system when simulated snow coverage is applied. Results also showed that SolarEdge system decreased tree shading losses from 17% to 13% in comparison to string-based system.

Keywords: Solar energy, Photovoltaic systems, Shading conditions, Power optimizers, Maximum Power Point Tracking, Bypass diodes, I-V characteristic

Acknowledgements

I would like to emphasize in this section that I am very fortunate to be working with a real company that has presented me with a project that has the potential to turn into a marketable solution. The completion of this project will leave me with invaluable experience and technical skills that will accelerate me through the transition into the workforce upon graduating. This project would not have been possible without the contribution of many different parts:

As I have been assigned to this project, sponsored by Vattenfall AB Research & Development, I have been presented with an incredible opportunity to gain real-world engineering experience. Many thanks to *Jonas Persson*, the Head of the Power and Technology department, and formal manager of my work for the warm welcome I received.

Throughout the completion of this project my project supervisor *Nicholas Etherden* has proven to be a valuable resource for me, given his credentials and his work experience. Nicholas advised me on every detail related to the project, he was always ready to help and contribute with useful suggestions and practical solutions all along the study. His work and dedication is worthy of praise.

I would like to thank *Mouaz Al Hamwi* for his vast background in the field and his absolute willingness to help along the entire project, and to *Jonas Wetterström* for his assistance in installing the needed hardware material and his unfailing support when complications arose.

I thank my supervisor and professor *Björn O Karlsson* at the University of Gävle, firstly for helping me to find this project, and secondly for his guidance since the early stages of my thesis. His broad knowledge and personal experience have demonstrated to be essential for the completion of this project.

I would like to express my gratitude as well to the whole Vattenfall R&D team in Älvkarleby, for welcoming me and making me feel at ease in the workplace during my stay. Thanks to *Monica Löf* for her help and disposition, and to *Anders Bohlin* for his support in the laboratory and for providing the equipment and components when they were required. I also appreciate the laudable effort of the electricians and mechanical engineers for the PV installation, roof set up and the experiments preparation.

I am grateful to *my friends* for their insightful comments and stimulating discussions, and for the shared experiences over the past years.

Finally, I must express my very profound gratitude to *my family* for providing me with wholehearted, boundless support and continuous encouragement throughout all my years of study and through the process of researching and writing this thesis. This accomplishment would not have been possible without them. Thank you.

Nomenclature

Symbols and variables

Symbol	Description	Units
α_s	Solar altitude	°
β	Tilt	°
δ	Declination angle	°
η	Efficiency	–
θ	Angle of incidence	°
θ_z	Zenith angle	°
ϕ	Latitude	°
ω	Hour angle	°
D	Distance	m
E	Equation of time	min
G	Global irradiance	$W \cdot m^{-2}$
G_b	Direct radiation	$W \cdot m^{-2}$
G_d	Diffuse radiation	$W \cdot m^{-2}$
G_r	Reflected radiation	$W \cdot m^{-2}$
$G_{b,n}$	Normal beam radiation	$W \cdot m^{-2}$
$G_{d,h}$	Horizontal diffuse radiation	$W \cdot m^{-2}$
G_h	Horizontal radiation	$W \cdot m^{-2}$
H	Height	m
I	Current	A
I_D	Diode current	A
I_{mpp}	Maximum power point current	A
I_{pv}	Photoelectric current	A
I_s	Series resistance current	A
I_{sh}	Shunt resistance current	A
I_{sc}	Short circuit current	A
K_B	Boltzman constant	$kg \cdot s^2 \cdot m^2 \cdot K^{-1}$
L_{loc}	Local longitude	°
L_{st}	Standard meridian	°
n	Day number	–
N	Number of	–
n_d	Diode ideality factor	–
P	Power	W
q	Electron charge	C
R_s	Series resistance	Ω
R_{sh}	Shunt resistance	Ω
T	Temperature	K
V	Voltage	V
V_{br}	Breakdown voltage	V
V_{oc}	Open circuit current	V
V_{mpp}	Maximum power point voltage	V

Abbreviations and Acronyms

Letter	Description
AC	Alternating Current
DC	Direct Current
MPP	Maximum Power Point
$MPPT$	Maximum Power Point Tracking
$NOCT$	Nominal Operating Cell Temperature
$NREL$	National Renewable Energy Laboratory
PSC	Partial shading conditions
PV	Photovoltaic(s)
STC	Standard Test Conditions

List of figures

List of tables

Table of Contents

1. Introduction

In this first section a background overview of the study is given. The studied problem is explained and motives for why the present work is a matter of interest.

1.1. Background

The world as we know today is based on the capability of humans to convert energy from one form to another. Energy is the capacity of a system to perform work, it is always conserved and it appears in many different forms. Humankind has made energy work for its own profit by converting it from one form to another form. The most prosperous and technologically developed nations are also the ones which have access to and are using the most energy per capita [1]. One of the biggest challenges in this century is tackling the energy problem. There is a supply-demand problem given that the energy demand is constantly growing, due both to the ever-growing world´s population and the increase in the energy consumption per capita as it is linked to the living standard of a country, which is also increasing [2]. The economic rise is a leading consequence of the above stated: due to the increasing demand from new growing economies, the energy prices have been significantly increased. A second challenge that humankind is facing is related to the fact that the energy infrastructure heavily depends on fossil fuels such as oil, coal and gas. Fossil fuels are nothing but millions and millions of years of solar energy stored in the form of chemical energy. The problem is that humans deplete these fossil fuels faster than they are generated through the photosynthetic process in nature. Therefore, fossil fuels are not a sustainable energy source, the reserves are disappearing as the rates of consumption are continuously growing. Another barrier is that it is technologically more challenging to get the fossil fuels out of the reserves currently left. Governments and companies are willing to take higher risks, like the Gulf of Mexico spill in 2010. A third challenge is that by burning fossil fuels we produce the so-called greenhouse gases (GHG) like carbon dioxide. The additional carbon dioxide created by human activities is stored in nature and its concentration in the Earth's atmosphere continues to rise [2]. Most scientists think the increase in carbon dioxide is responsible for the global warming and climate change, which can have drastic consequences for the habitats of many people and organisms. Furthermore, the energy conversion from fossil fuels to electricity has no greater than 50% efficiency [3]. Hence, it is important to look for alternative energy sources, like fuel cells, nuclear power, or renewable energies.

Renewable energies grant reduced carbon footprint and low or non-existent GHG emissions compared with fossil fuels. More specifically, the use of solar energy is counted as an unlimited source of energy, and it has been since the beginning a subject of extensive research due to the various advantages it offers [4]. Solar energy can be converted into heat, electricity, and chemical energy. The phenomenon that occurs when solar light is directly converted into electricity is called photovoltaics (PV), and this is possible thanks to devices based on semiconductor materials. The global electricity demand in 2018 was mostly covered by fossil fuels and nuclear power, accounting for 72% of the total share. Renewable energies covered the rest with hydropower as

the largest provider therein, with a share of 17%, followed by wind power which accounted for 6%. PV represents around 2.6 % of the global electricity demand and 4.3 % in Europe [5].

Solar energy can ensure a more rapid expansion than other technologies because of its availability and abundance worldwide. The energy coming from the Sun is 10 000 times greater than the world's energy consumption [6]. PV systems also have the advantage of offering flexibility and adaptability in their installations. They can be installed concentrated in vast solar farms for energy production on a large scale, in the same way as hydro power plants, nuclear plants or wind parks are constructed. These constructions require governmental involvements and big investors. However, solar energy has the unique advantage over other renewable energies of allowing the installation of decentralized systems, for residential or commercial buildings, off-grid and autonomous PV applications, etc. Due to this, among other reasons, the use of photovoltaics in the electric power generation has undergone a major increase over the past years.

The global annual PV generation reached 100 GW peak in 2018, and it has been increasing by 40% in reference to the previous year. More than 20 years ago the main PV module production was led by the United States, Japan and Europe. The trends for the US have experienced a continuous decrease, while Europe remained constant and Japan became the leader in this market. In the last decade, thanks to massive investments of the Chinese government, the largest manufacturer of PV modules nowadays are China and Taiwan, responsible for 80% of the global PV module production. [5], [7]

PV installations have been growing exponentially at a rate of 25% per year throughout the last decade due to subsidy policies which were especially popular in Germany, Spain and Italy by the year 2008. The European market share increased up to 80%, and soon thereafter the Asian PV market started to increase very rapidly as well. The global installed cumulative capacity for PV crossed the 500 GW mark in 2018, 100 GW more than in the previous year. China is the leader in terms of total cumulative capacity with 176.1 GW installed, followed by the United States with 62.2 GW, Japan with 56 GW, Germany and India, having the latter one 32.9 GW installed. The European Union accounts to have 115 GW, where Germany has nearly half of the share with 45.4 GW, followed by Italy, United Kingdom and France. [5]

The growth of PV in Sweden is a leading cause of reduced technology costs and government funding for micro producers [8]. PV electrical generation share in the market is rather small in comparison to the total yield, accounting for only 0.2% in 2017. Nevertheless, installed capacity has been increasing up to 80% per year, and also the average installation size. [9]

Yet the vast research done on the field, and the knowledge acquired throughout the years, the calculation and evaluation of PV power has been hindered not only by the fact that just a small fraction of systems declare their production on a regular basis, but also by the lack of accessibility to the metadata [10]. Nevertheless, PV is certainly a well-known technology and the studies conducted have by far provided extensive information about the effects that influence their performance.

One of the most important factors that affect PV production is, among others, the shading effect, and it is crucial to diminish its negative impact on PV production. Shadows over a solar cell, module or array of solar panels lowers the current and voltage of the entire system, rendering a limited output and decreasing the overall system's efficiency. [11]

One way to tackle this issue is to introduce the use of power electronics in the electrical configuration of the PV systems. The proposed study investigates the performance of two PV systems with different power conversion setups, including DC power optimizers and string inverters. It compares the shaded performance of optimizer-based and standard PV systems, as well as the shaded performance of each system relative to its own unshaded performance. Findings are utilized to verify gains associated with optimizer-based PV systems and support product marketing. This study was presented by Vattenfall AB and carried out at its Sweden´s largest facility – Vattenfall Älvkarleby laboratory.

1.2. Literature review

Research on the topic has been done to gain a better understanding of what is studied herein, to serve as a vast background for decision making throughout the course of this report and to provide awareness of PV on both a global and a regional scale.

Many external factors can affect a PV system's energy output, such as solar irradiation, temperature, solar incidence angle, dust, shade, etc. Saint-Drenan et.al conducted a study of the performance of PV systems to find out the most influential parameters affecting PV output generation. There are four of them: tilt and azimuth angle of PV modules, installed capacity and overall efficiency. Additionally, shading has a crucial impact on the PV yield, although little research has been done on it [12]. The four parameters listed above refer to a PV system's performance under light conditions, but the results are substantially different when shade is projected on the modules.

Shading is an aspect that generally cannot be avoided since any object close enough to the building in which PV panels are installed can create a shadow due to the apparent movement of the Sun through the day over the year. Shade causes a decrease in the current and voltage given by a solar panel, and hence in the energy delivered. Under shadowing conditions a PV system can have large energy losses and even small shadows can noticeably affect the energy yield [13].

Besides the shadow generated by trees, buildings or nearby objects, clouds and particles in the air will also affect the irradiance a PV system is receiving. A common approach to take climatic effects into consideration is to use special radiation measurement instruments to obtain the actual solar radiation that reaches the Earth. The longer time this data has been gathered for, the more accurate it will be. There are certain locations worldwide where it has continuously been collected, such as the National Renewable Energy Laboratory (NREL). Unfortunately, these location are very small in number than what would be desirable [14].

Within a PV array that is partially shaded, the solar panel providing the minimum yield will limit the overall system's production, and this will have a greater or minor impact depending on the configuration of the modules. The connection of panels within an array is a widely used technique to increase the PV production and efficiency, being the most common configurations listed as follows: series-parallel, bridge-linked, and total cross-tied. The latter has the most satisfactory performance under shading conditions, resulting in less operation losses [15]. The study presented in [16] aims to solve this problem with the simulation of PV modules under various shading patterns for the three configurations of PV arrays above introduced. Results shown that for shading scenarios covering 50% or more of the total area of a module, the reconfiguration of the arrays was not advantageous since it only brought a gain of 5% in the total power output. It must be noted that, in practice, the wiring of solar panels is subject to the inverter connected to the system, depending on the input voltage and current coming from the PV installation.

In order to achieve an increased production and efficiency, Maximum Power Point Tracking (MPPT) techniques at the level of individual cells are required, and they are of indubitable importance namely under partial shading conditions (PSC) [11]. MPPT looks for the maximum power that can be delivered by a solar module or array. It is known that without appropriate monitoring of the PV system MPP, it is not possible to extract the maximum power of a PV system, and this fact is emphasized when light is not received uniformly, for example in case of shading conditions. MPPT models are based on the combination of a suitable control technique and the adjustment of the duty cycle of a DC/DC converter. The control technique is implemented in accordance with various algorithms, such as: incremental conductance, perturb and observe, constant voltage. Yet crucial, it is still a challenging problem nowadays. In [7] a review of different MPPT techniques is approached, concluding that the metaheuristic optimization algorithms are the best methods, performing better than classic, fuzzy logic control based and artificial neural network based MPPT techniques.

Shading losses can be mitigated with bypass diodes, used in the internal electrical configuration of a PV module or in parallel with a solar panel. The configuration design has a big influence on the likelihood and severity of hot spot occurrence in any module of the PV array [4]. Some authors have investigated the minimum bypass diodes that must go within a PV module based on the maximum capacity to dissipate power of the solar cells without being damaged. The study [4] proposes an expression to estimate the maximum number of solar cells that should be protected by a bypass diode, concluding, given certain cell parameters, in no more than 16 cells. However, this number heavily depends on the specifications of each solar cell, and the uncertainty related to degradation or the manufacturing process.

An effective solution to keep track of the MPP at a module level to achieve a better PV system's performance and a higher overall production is the use of power optimizers. The independent study presented in [17] shows the behavior of PV topologies under partial shading scenarios performed in a standardized NREL case. It compares the solution provided by SolarEdge system with power optimizers and central inverter, with the SMA string inverter and the Emphase

micro-inverter systems. Results showed that SolarEdge outperforms SMA and Enphase systems under any shading conditions, especially when compared to SMA. SolarEdge system demonstrated a 2% energy gain for light shade and up to 8.5% under more severe shading in comparison with the string inverter system.

The method described in [18] presents the procedure to scientifically measure and evaluate the shading effect on solar panels with and without power optimizers. To emulate the yearly losses on residential roof PV systems due to shading, three different scenarios are studied: light, moderate and heavy shading. Each one of them has its corresponding weighting factor based on their likelihood of occurrence, from the most probable scenario – light shading - to the least – heavy shading. Direct shading is applied on two different PV systems placed one next to the other using a semi opaque fabric mesh: a 50% open vinyl/polyester fabric with 37% transmittance. Results showed that the system with optimizers had higher yield as shading increased. However, it should be noted that although this type of technique – direct shading - allows greater control over the experiment, it is not entirely realistic, as shadow patterns are accompanied by diffuse radiation most of the time, and have a variable nature depending on the time and region.

The information above gathered provides the reader with an overview of the situation of PV systems from a general point of view and within the Swedish market, and it also endorses the motivation of this project.

1.3. Aims

This report targets the issue of the shading effect on PV systems and its impact on their power output, as well as the gains associated to optimizer-based PV systems under such conditions. It is meant to develop and validate a test procedure to estimate and evaluate shading losses. It is expected to broaden the knowledge on the subject as there are many concerns yet to be studied. From a sales perspective this work intends to provide information regarding the optimal orientation to install the PV systems and to support the solution with power optimizers.

Different hypotheses are taken into consideration throughout this project and will be presented in their corresponding sections. As for the delimitations, this work focuses on the study of two residential PV systems, a string-based system and an optimizer-based system. The conducted experiments are designed and prepared to reproduce as accurately as possible the real scenarios aimed to study. Data is collected for the months of April to June. As far as limitations of the project are concerned, the resources, instruments and source of data employed, and the validity of the obtained results are mentioned in the Discussion chapter.

1.4. Approach

The present study was performed based on an experimental approach, and a quantitative research was done to analyze the obtained results. Comparisons between the different scenarios and experiments support the conclusions drawn from the analysis.

2. Theory

Theoretical background and elementary fundamentals on which the present work is based are presented herein. Firstly, the basic theory behind photovoltaic energy is introduced, followed by the working principles of a solar cell. Afterwards, important concepts related to PV systems are explained and the factors affecting their performance, including the shading effect.

2.1. Photovoltaic Energy

Sunlight reaching the Earth surface is often referred as the irradiance, which is the power received by a surface per unit area. This global irradiance over a tilted surface such a solar panel can be divided into three different components:

$$G = G_b + G_d + G_r \quad (1)$$

$$G_b = G_{b,n}\cos(\theta) \quad (2)$$

$$G_d = G_{d,h}(1 + cos(\beta))/2 \quad (3)$$

$$G_r = \rho_g G_h(1 - \cos(\beta))/2 \quad (4)$$

G_b is the beam radiation, and it is the direct radiation towards a tilted surface, which is governed by the normal or perpendicular component ($G_{b,n}$) and its angle of incidence (θ).

G_d is the diffuse radiation, and it is calculated with its component towards a horizontal surface ($G_{d,h}$) and the tilt of the surface from the horizontal (β).

G_r is the reflected radiation and it is herein calculated, for simplicity, according to the isotropic model, which assumes that the diffuse radiation has the same intensity from the entire sky. The parameters ρ_g and G_h are the reflectants of the ground and the total radiation towards a horizontal surface.

The mechanism in which solar energy is directly converted into electricity is called the photovoltaic effect. This is done by the so-called solar cells, which are electrical devices made of semiconductor materials. These materials are doped to create a p-n junction, which has the same functionality as a single diode since it allows the electrons to flow only in one direction. Sunlight photons enter the solar cell and are transmitted into the absorber layer, where both positive and negative energy carriers are excited by this incoming energy. The energy carriers are diffused, sent to the depletion regions and collected at the contacts of the solar cell. These contacts are connected with a load through which the negative charged carriers – the electrons - flow and generate electricity. Both energy carriers are then recombined in the solar cell, and so the process begins again. PV technologies can be categorized based on the semiconductor material used as absorber layer in the solar cell. The four main types are crystalline, thin film, compound semiconductor and nanotechnology, which are briefly described below [19].

- Silicon crystalline structure is the first generation is the most dominant, representing nearly 90% of the market [20]. It can be further sub-divided into mono-crystalline, poly-crystalline, and Emitter Wrap Through cells. These cells have large initial investments but rather small maintenance and operation costs, because of the use of pure bulky materials. Looking for a module cost reduction the market moved towards the second generation of PV technologies.
- Thin film technology is the second generation and it accounted for 10% of the market in 2015 [20], but their market share has since then diminished. They present a significant reduction in the manufacturing costs due to the use of less photovoltaic material, which also leads to lower efficiencies than the previous group. In this group it is worth mentioning the Cadmium telluride and the Copper Indium Gallium diselenide types of cells, which are the most efficient ones within this group, achieving up to 20%.
- Compound semiconductor cells are multi-junction based and they are the most efficient solar cells nowadays. They have proven in laboratory tests to achieve efficiencies of up to 44%, obtained with a metamorphic triple junction in 2012. These solar cells are used in concentrator PV technology and in space applications.
- Nanotechnology components introduced could control the energy band-gap and would then absorb more sunlight, providing versatility, and hence improving the conversion efficiency. Some of these structures are nanotubes, Quantum Dots, and "hot carrier" solar cells. This type of cell has not been commercialized to date.

A solar cell can be represented with its equivalent electric circuit. Depending on how accurate they are and the parameters taken into account, various models have been developed to emulate the behavior of the solar cell. The most widely used is the single-diode model, although there have been developed other more sophisticated designs, such as the two-diode model, which additionally considers the effect of the recombination at the space charge region as well [4]. Fig. 1 shows the single-diode model with series and shunt resistance, which aim to consider the effect of the contacts and the leakage currents, respectively. The mathematical equations used to model the current in this case are presented as follows: [21]

$$I = I_{pv} - I_D - I_{sh} \tag{5}$$

$$I = I_{pv} - I_s\left(e^{\frac{q(V+I\cdot R_s)}{n_d\cdot K_B\cdot T}} - 1\right) - \frac{V + I\cdot R_s}{R_{sh}} \tag{6}$$

Where I_{pv} is the photoelectric current, I_D the current through the diode, I_{sh} the current through the shunt resistance, I_s the current through the series resistance, n_d is the diode ideality factor, K_B the Boltzman constant (1.38062E-23 $kg\cdot s^2\cdot m^2\cdot K^{-1}$), T the solar cell absolute temperature, q the electron's charge (1.602E-19 C), and I, V the output current and voltage of the solar cell.

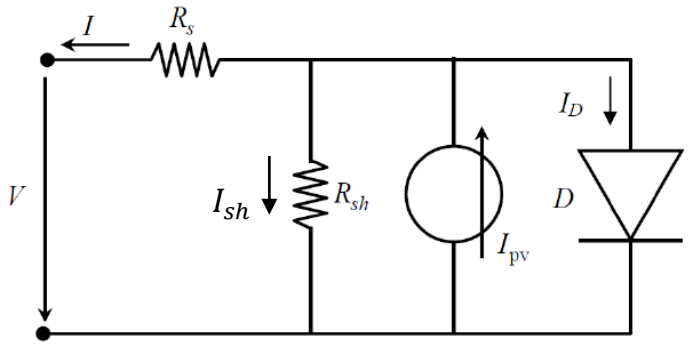

Fig. 1: Equivalent circuit of the single diode model for a solar cell [22]

Solar cells are usually wired in series to form modules, which are typically manufactured for a 60 or 72-cell configuration corresponding to 1.6 or 2 m^2 panels. It is common to find bypass diodes in the junction box, which are meant to protect 20 or 24 of these cells in series. The electrical unit of cells covered by a bypass diode is sometimes called submodule. The mechanically and electrically integrated assembly of modules and side components is a PV array, and it is a DC power supply unit. Fig. 2 shows the above cited combinations:

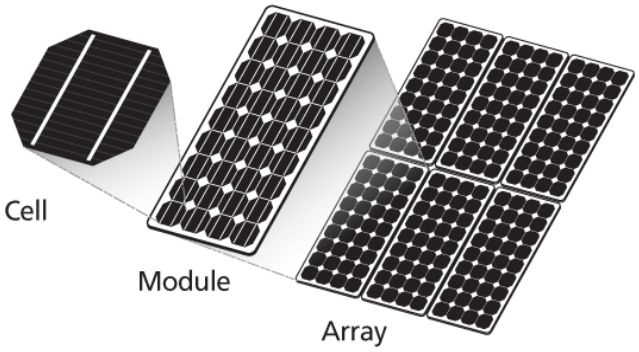

Fig. 2: PV cell, module/panel and array/system [22]

Note that solar module does not always mean the same as solar panel, depending on the nomenclature adopted. However and for simplicity, they are referred interchangeably in this study.

2.2. I-V characteristic

The relation between current and voltage of a given solar cell or module is represented by the so-called I-V curve, from which the P-V curve can be obtained. These are defined for a unique set of temperature and irradiance conditions. The former presents all the possible combinations of its current and voltage outputs for a fixed irradiance and cell temperature. The latter is the Power-Voltage curve and it is the result of the product of the output voltage and current. Since the I-V curve of a solar module is no other thing but the addition of the I-V curves of the individual solar cells which compose the panel, the theory behind it applies equally for both.

This curve can be theoretically determined from the above mathematical equations (6) that model a solar cell. In practice, the I-V characteristic is obtained with a measurement instrument which principle lies in a variable resistor in series with the object under test. Both output current and voltage are measured as the resistor value varies from 0% to 100%, situations corresponding to a short circuit and an open circuit, respectively. The key points in the I-V curve are the short circuit current, the open circuit voltage and the maximum power point. The solar cell or module yields its maximum current when there is no resistance in the circuit, meaning that there is a short circuit between its positive and negative terminals. The output voltage is zero, and the maximum current is called Short Circuit Current (I_{sc}). On the other hand, the maximum voltage occurs when the resistance is maximum and therefore the current is zero, i.e. there is an open circuit. This voltage is known as the Open Circuit Voltage (V_{oc}). The MPP is the point of maximum power output, and it occurs when the product of voltage and current give the highest yield. This point is critical since it determines the production and efficiency of the system, and it is determined from the P-V curve at its highest peak. This can be seen in Fig. 3.

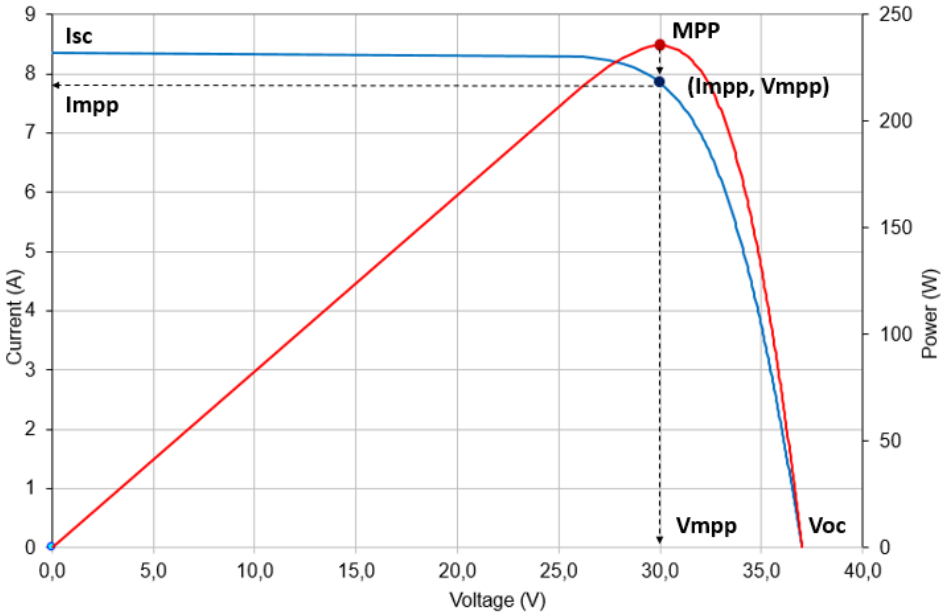

Fig. 3: Generic I-V characteristic (blue) and power graph (red) of a solar module

As the I-V characteristic is given for a specific irradiance and temperature, the curve varies for different values of these factors, as it can be observed in Fig. 4 and Fig. 5. The effect of the isolation and cell temperature in the current and voltage is therefore reflected in the power output. The irradiance received by a solar cell or module strongly affects current values in a directly proportional way, that is, the intensity and therefore the power increase with the irradiance.

Fig. 4 shows the impact of irradiance in the I-V characteristic and its corresponding power graph.

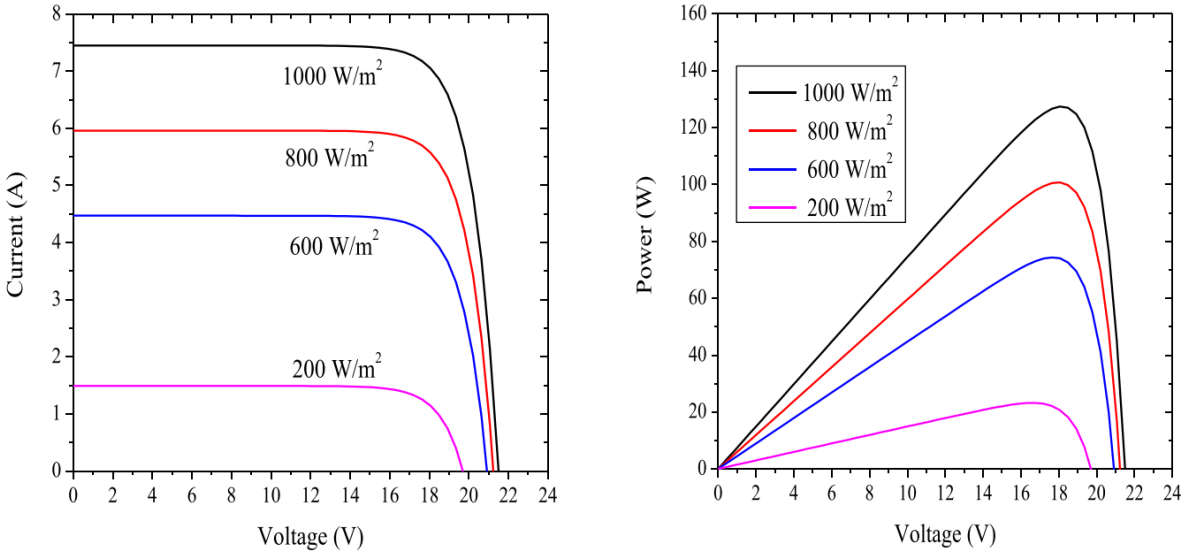

Fig. 4: I-V and P-V curves at different irradiance levels for a given cell temperature [23]

On the other hand, increasing the cell temperature negatively affects the power output by means of reducing the voltage of a solar cell or module. As it can be seen in Fig. 5, the higher the temperature, the lower the voltage and therefore the power. Nevertheless, the impact of the cell temperature in the power output is not as severe as the effect of low irradiance.

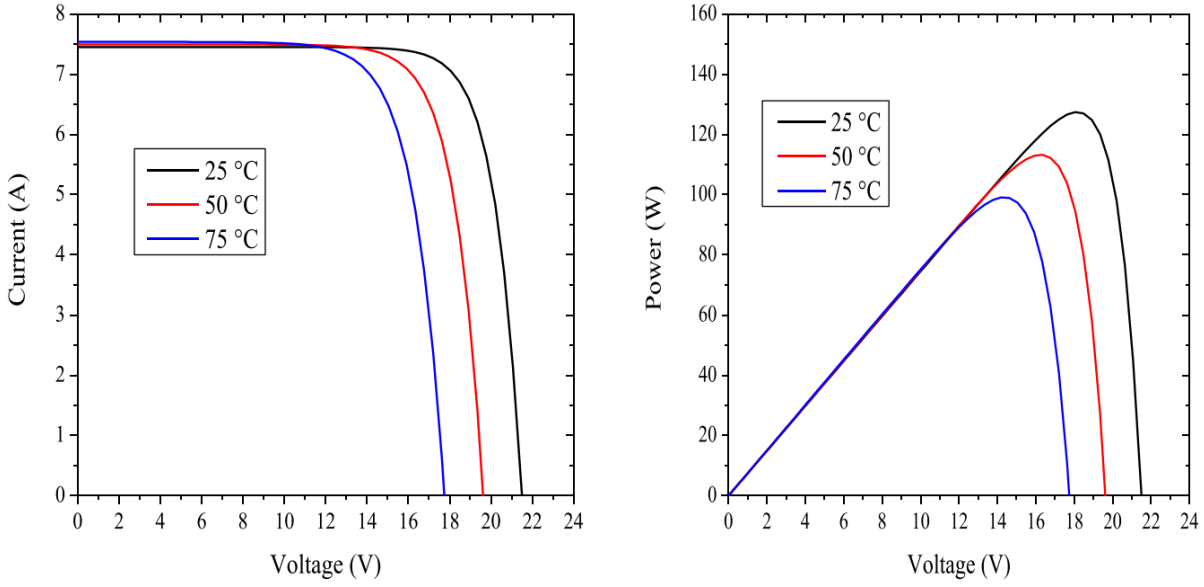

Fig. 5: I-V and P-V curves dependency with cell Temperature for a given irradiance [23]

It could be said, consequently, that the optimum performance of a system requires the highest irradiance and the lowest temperature possible. For comparison, power rating of a reference solar cell is therefore given at a standard irradiance and temperature, denoted Standard Test Conditions or STC.

PV cells can be connected in series or parallel, as it can be seen in Fig. 6. Based on electrical principles it is known that a series connection requires the same current through the elements,

while the voltage drop will depend on the resistance that each element opposes to the flow of electrons. On the other hand, a parallel connection of components demands the same voltage between terminals, whilst the current through each string will be conditioned by the existing resistance. A single solar cell can produce up to 0.65 V, and the current through it will depend on the irradiance received and the electrical configuration adopted. In order to produce higher voltages, solar cells are series connected to form modules. Solar panels also have their own values of maximum current and voltage that they can deliver, and their I-V characteristic will depend on the electrical internal configuration of the solar cells comprised within. Normally, the voltage at which a solar panel works moves towards 30 V. Since this gives a rather low DC power level to be effectively converted into AC to transfer to the grid, solar modules are thus connected in series to deliver a higher voltage.

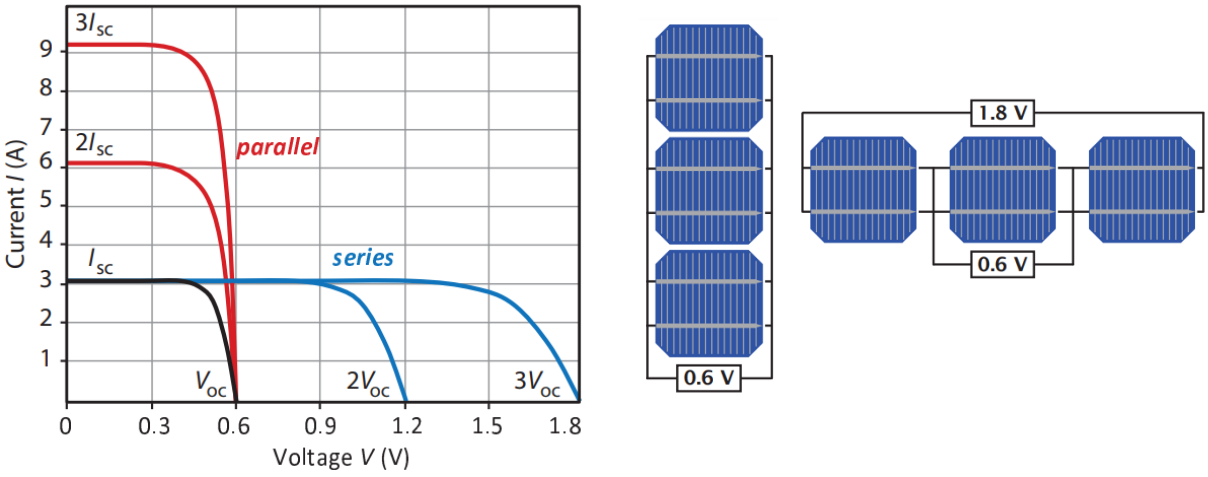

Fig. 6: I-V curves of solar cells connected in series and parallel [23]

2.3. Shading effect

The performance of PV systems depends not only on the solar irradiation received and the temperature, but also on their configuration and shading. Shading is present in most of PV installations due to clouds, soiling, neighboring trees, buildings, or even objects placed next to the solar modules. The shading effect is strongly detrimental to the overall production, as it causes energy loss in the conversion and also non-linearity on the I-V characteristics [24].

The shading effect has a huge impact in the output energy itself. As explained in the previous section, solar cells are wired in series to form solar panels, so the voltage of all cells is added up and, along with the output current, delivered. The shade of a single cell would cause a reduction of the current through the string, and hence of the power delivered. This behavior can be observed in the I-V characteristic and the corresponding power graph of the shaded PV module, and of the PV array.

As it is discussed later on, it is not possible to state that it is always better to concentrate the shade on one string rather than equally distribute it on all the strings of the array. It is nevertheless

observed that when the percentage of shaded modules is high – for instance up to 25% - it is better for the overall production if the shading is concentrated on a string. In this case, the voltage corresponding to the MPP is fixed to the value without shade. As for when the percentage of shaded modules is limited – around 10% - it might be better for overall production when shading is evenly distributed, even if there is the disadvantage of reducing the voltage corresponding to Maximum Power.

Most of the times, shading patterns are unpredictable, changeable and non-uniform. This is what is referred in this report as partial shading conditions, and it brings many problems along with it. PSC affect tracking algorithms and it can be extremely damaging for the solar cell materials. As it is known, MPPT techniques provide the best outcome for uniform illumination, and this non-uniformity cause by shading patterns severely affects the output PV production. This effect is stressed with fast changing shading patterns, because there will be numerous local MPPs and they will change as fast as does the illumination over the panels [11].

Besides, the shading effect can be very harmful for the semiconductor materials which solar cells are made of. When a cell is shaded while the remainder in the module are not, part of the power generated by the unshaded cells is dissipated by the shaded one as heat. If this power exceeds the maximum power which can be sustained by the cell, it can lead to concentrated hot spots which can lead to irreparable damages to the PV module.

Hot spots appear under PSC or as effect of mismatch. If one module has shade on part of it but the rest is unshaded there will be different current through the cells: the cells that are absorbing more irradiation will have higher current whereas the shaded ones will be limiting the current through the string. For this reason, the cells with higher current have to dissipate that power in some way, because they are wired in series and therefore the current has to be the same over the entire string. This power is dissipated in the form of heat, rising the temperature of the cell. This is extremely harmful for the solar panels and it is one of the main reasons of the degradation of their materials, rendering a premature lower efficiency.

When a solar cell in a module is shadowed, it might be reverse-biased by the unshaded cells. The current through a shaded cell is lowered due to less received irradiance. This current drop causes the solar cell to enter in the negative voltage region, as it can be seen in Fig. 7. If the voltage reaches the breakdown voltage, the current grows exponentially and so the power dissipated does. For multicrystalline silicon solar cells, breakdown voltage is found to be around $V_{br} = -13$ V, which is lower than expected from theory (−60 V) [25]. When the cell is working in reverse bias, it will act as a load and will dissipate power instead of generating it. Also, since the current will be flowing in the opposite direction into this cell, the rest of the series connected cells will not see any current since their diode nature only allows to receive forward current, and an open circuit appears.

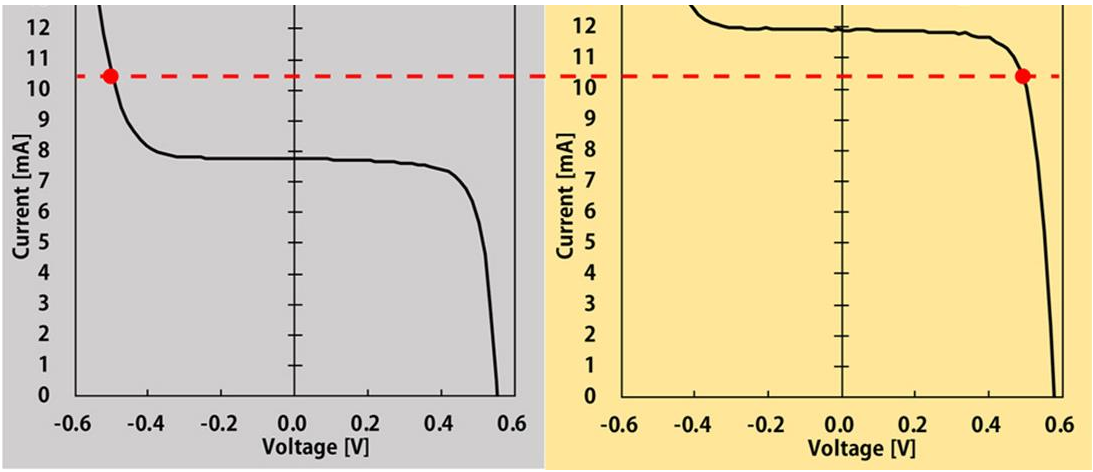

Fig. 7: I-V characteristic of a solar cell under shaded (left) and unshaded (right) conditions [26]

The breakdown voltage can also be utilized as a useful tool to know the maximum number of cells that can be protected by a bypass diode without being damaged. If the value of $V_{br} = -13$ V is taken, and given that each cell gives 0.65 V, then it results in a maximum of 20 cells per bypass diode, which is a typical solution adopted by PV module manufacturers, as it is also the case of the main systems under the scope of this study.

The PV array layout and the use of bypass diodes on PV modules have a decisive influence in the possibility of hot spot apparition. [4]

2.4. Bypass diodes

When a cell is shaded the current through it decreases accordingly with the intensity of the shade: the more concentrated the shade, the more intensity reduction. Solar cells arranged in series are then limited by this lowest current dictated by the shaded solar cell, causing the power reduction of the entire solar panel supposing that there are no bypass diodes. The use of these additional p-n junctions allows for isolation of groups of solar cells within a module. In case of shade and thus current reduction, the bypass diode would start working and the set of cells would be bypassed, permitting the rest of the unshaded cells to operate at their MPP. Despite the extra cost, the use of bypass diodes is a widespread application in the industry as a compromise between protection and increased cost.

A shaded panel of a non-uniform illuminated PV system can be submitted to a negative voltage [4]. The use of bypass diodes is a common practice to avoid cell breakdowns and to prevent the hot spot formation in partial shadowing conditions of work. Bypass diodes are connected in parallel to a certain number of cells within a PV module, for instance every set of 18 cells [27] or in parallel with a PV panel. Note that the equivalent electric circuit of a solar cell must be altered to count the effect of partial shading, because the cell will work in its reverse characteristic. For this situation, Bishop's model – which includes the effects on the shunt resistance current term - is still the most broadly used, albeit it only refers to the study at a module-level and does not consider the shading effect on a complete PV array [4].

If the shade is enough to lower the current at a level that the cells in the string enter the negative voltage region, the bypass diode starts operating because it is connected with opposite polarity to the string of cells in parallel. This is given by Equation 7: if the shading is more than the following ratio, the diode starts functioning.

$$\% \, Shading \geq 1 - \frac{I_{mpp}}{I_{sc}} \tag{7}$$

The specific ratio at which a solar cell becomes a power consumer instead of producer varies depending on the type of cell and bypass diodes used, but typically a value of 20% is enough to activate the bypass diode.

Under normal operation the current will normally flow through the cells because the diode only allows to let the current pass in one direction, and since bypass diodes have opposite polarity they would not conduct. If there were no bypass diodes, the cell would reach the breakdown voltage, where the current reaches extremely high levels, and that would cause the rapid degradation of the affected cells due to the apparition of hot spots, for example. Fig. 8 shows a PV panel of 60 cells with three bypass diodes protecting a string of 20 cells. Enough shade on a single cell in one of the circuits results in the bypass of the current of one 20 cell string, meaning that this circuit does not produce any power.

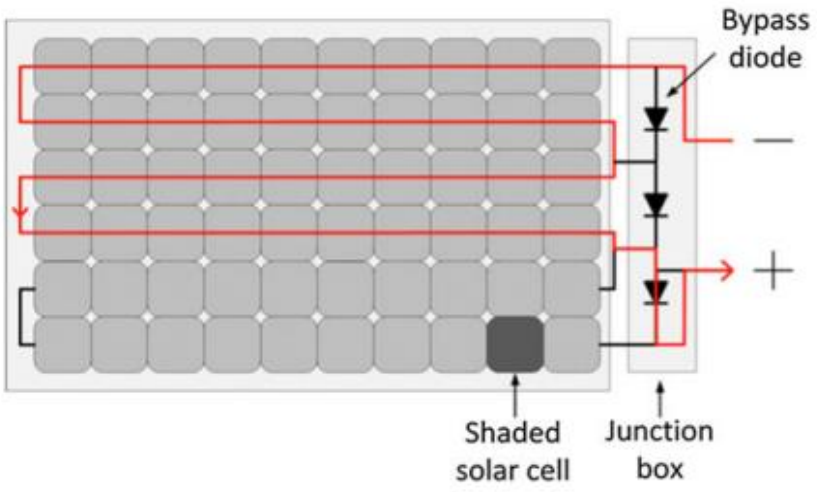

Fig. 8: PV module with one shaded solar cell [28]

As an example, it is considered the case of a circuit of 20 cells in series with its bypass diode, as it can be seen in Fig. 9. For unshaded conditions, the current is 8 A and the voltage of each cell 0.6 V, giving a total circuit voltage of 13 V, as shown in Fig. 11 (a and b).

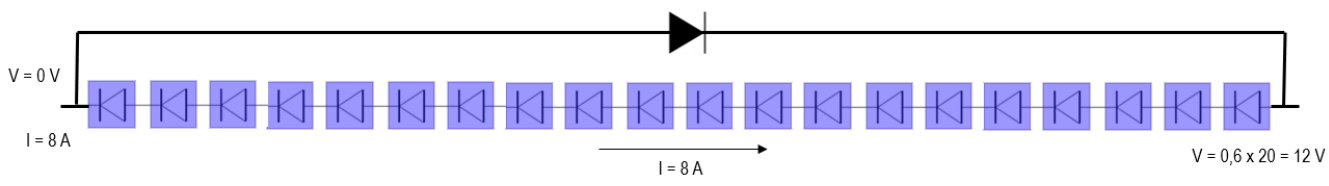

Fig. 9: Circuit of 20 cells of a module and its bypass diode, unshaded

As it is done in the experiment with the fabric mesh (see section 4.2), 60% of the three circuits are shaded. In this example 12 cells, which corresponds to 60% of a circuit, are shaded 70% of their area. The current through the string lowers down to 30% of the incoming current, and the rest of the current is redirected through the bypass diode. The illuminated cells give as much as 0.6 V each, or 4.8 V in total, whereas the shaded cells are reverse-biased and work at -0.45 V each. The new operating point is shown in Fig. 11 (c and d). This results in an open circuit, and the only voltage drop occurs in the diode, which has 0.65 V as default. The power dissipated by the shaded cells is of 1 Watt of heat, and in turn the diode produces 3.6 W of heat. Fig. 10 presents a schema of this situation.

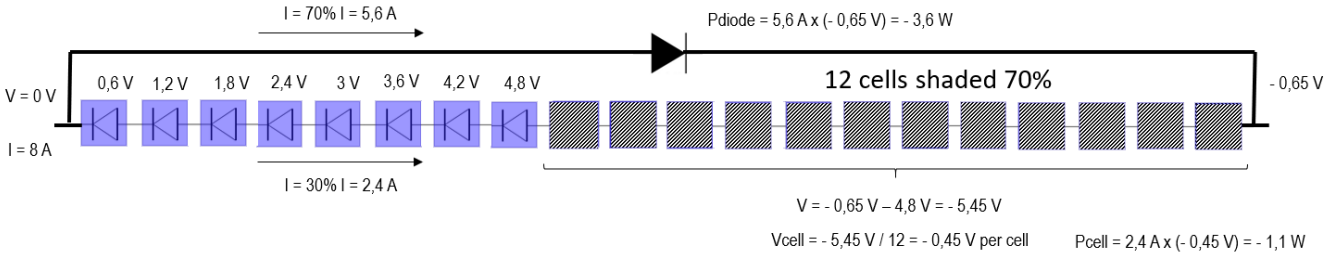

Fig. 10: Circuit of 20 cells of a module and its bypass diode, 60% of the circuit shaded 70%

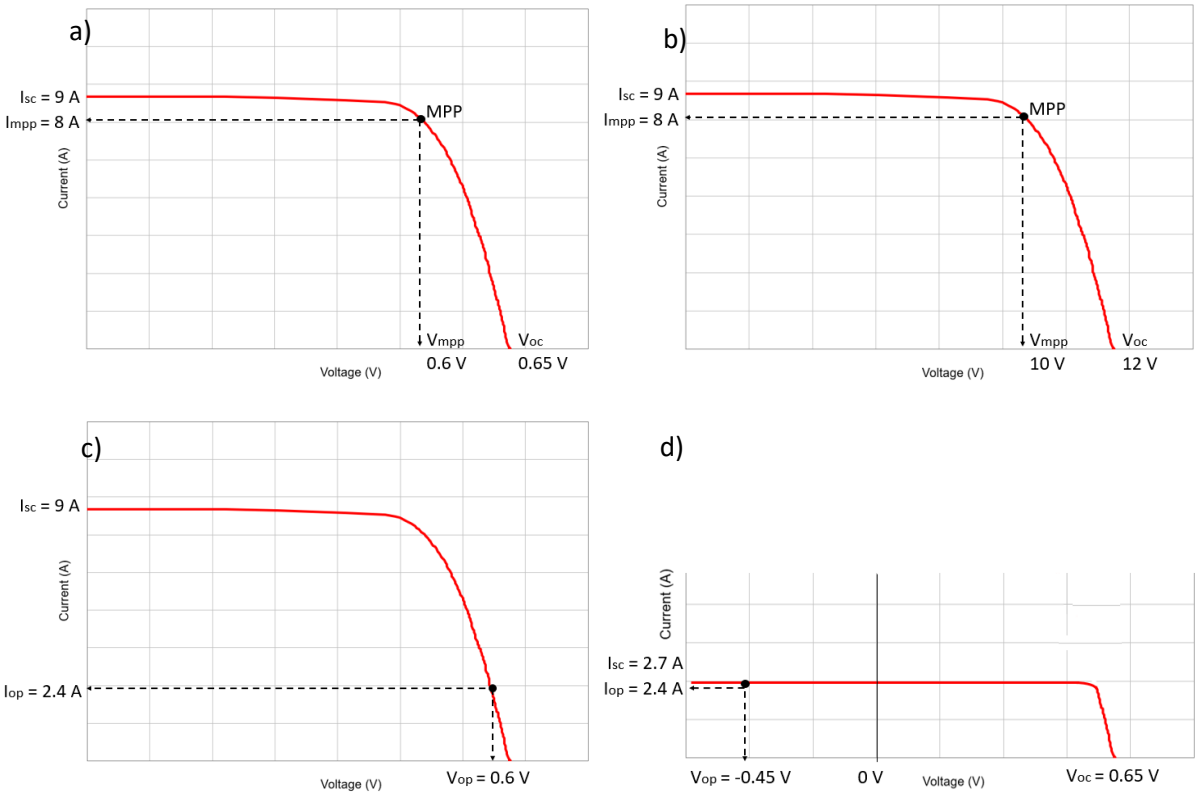

Fig. 11: I-V characteristic for a) unshaded single solar cell, b) unshaded 20 cell circuit, c) operating point unshaded cell, d) operating point shaded cell

2.5. Power optimizers

The DC production of PV modules is maximized with the use of a device implemented with MPPT techniques, before being converted into AC power in the PV systems inverter and sent to the grid. Traditionally solar inverters come with an MPP tracker for one or multiple strings integrated in a central inverter. The problem of this method is that if one single module is yielding less power than the rest, it will affect the overall output of the system, because the modules are all connected and will have the same current and voltage working point from the MPP-algorithm. Certain module connections are more advantageous than other for PSC, but in any case, the shading effect will affect the output.

An alternative solution is to track the voltage and current of each module separately, obtain the individual MPP of every module. This can be achieved either with micro-inverters that transform the DC directly to AC at module level, or with power-optimizers. As the cost of micro-inverter solution is higher, power optimizers are much more common [29].

SolarEdge was founded in 2006 and sold its first inverter in 2010. It has quickly become the world's second largest PV manufacturer and largest manufacturer in countries with single phase like US. SolarEdge exclusively uses power optimizers that work alongside the inverter they are linked to. This practice guarantees that the total input DC voltage to the central AD-DC inverter is always the same and it is compliant with the inverter admitted voltage range.

As for series connected modules, the same current is required to flow through the string. In shading scenarios this current over the shaded module is lowered to a certain extent. In the case of string inverters this would result in the decrease of the current through the string and therefore of the total power output. In turn, optimizers would increase the outgoing current from the shaded module by means of lowering its voltage drop. The current delivered from shaded modules that goes into the common string would still match the current level of the illuminated modules, only the voltage drop is less. This grants more overall power delivered to the central inverter.

The use of such devices grants an advantage in the face of standard designs only in the case of PSC, as it is explained in the Discussion chapter. They also serve for the correction of mismatched modules, since they track MPP individually. Note that for situations of no shading both systems would harvest equivalent output because they would have identical I-V and P-V curves, and the MPP tracked would be the same. Likewise, as for when all the solar panels are shaded they also have the same curves and thus the same production would be obtained. In these scenarios power optimizers would not entail any benefit, and the difference between the systems would then lie on the efficiencies related to the inverters, optimizers, mismatched modules, wiring, temperature, non-uniform illumination, etc.

3. Method

This section aims to give a detailed description of the experiment, from the materials and tools employed to the methodology followed to achieve the results.

3.1. Study object

At Vattenfall R&D laboratories in Älvkarleby (Sweden) two similar residential PV systems have been placed next to each other. One traditional string-based inverter system as sold by Vattenfall up to mid-2017. The other is an optimizer-based system. For this study the objects under test were subjected to similar artificial shading with the goal to quantify the reduction in shading losses under partial shading conditions. The arrays are composed of two rows of modules connected in series, with either 6 or 8 modules for each row. The smaller system has a string configuration, meaning all the modules are connected in series and the total output is processed by an inverter which keeps track of the overall Maximum Power Point (MPP). Therefore, shading one module will affect the overall output of the system. The other one includes an optimizer attached to every module, which allows to track the MPP of each one of the modules separately.

3.2. Materials

The PV modules employed in this experiment are JKM270PP-60 Poly-crystalline from JinkoSolar for the PV system with optimizers, which is the one currently sold by Vattenfall AB to residential PV customers, and YL275C-30b Monocrystalline from Jinglisolar for the string connected system, sold until mid-2017. The optimizer-based system consists of 16 solar panels in series, with a maximum rated power of 270 W peak, and it has P300 SolarEdge optimizers attached to each module of the arrays. The string-based system is composed of 12 modules connected in series, with a maximum rated power of 275 W peak. Note that the maximum rated power is at Standard conditions (STC)[1]. Both types of modules have three integrated bypass diodes in parallel with every 20 cells out of the 60 that constitute a solar panel.

Both systems are sending energy to their respective grid-connected inverters. The arrays are equipped with a 4 kW SolarEdge three-phase inverter for the system with optimizers and a 3 kW Fronius inverter for the one with string configuration. These devices have the function of processing the energy coming from the solar panels and transforming it into AC power to match the grid voltage, waveform and frequency. They also need to be in synchronism with the grid, meaning that the phase of the AC signal coming from the inverter is in phase with that of the grid. As far as safety standards are concerned, they automatically disconnect from the power line in case of failure, and they deliver a marginally higher voltage than the grid to make the energy flow smoothly outwards the solar array. The current installation of inverters is shown in Fig. 12.

[1] STC: Standard Conditions at 1000W/m2 irradiance, 25°C cell temperature, AM1.5g spectrum according to EN 60904-3

Fig. 12: Current installation of invertres in the electricity room at Älvkarleby: SolarEdge (left) and Fronius (right)

A calibrated reference solar cell is utilized to measure the irradiance of the PV systems. It is located between the two systems, with identical orientation and tilt (see Fig. 17). This is a high-quality irradiance sensor with an irradiance output signal of 0 to 1.4 V covering a 0 to 1400 W/m^2 range (Fig. 13).

Fig. 13: SolarEdge direct irradiance sensor (SE1000-SEN-IRR-S1)

The inverters and the reference solar cell send the data via ethernet through a gateway communication (see Fig. 14).

Fig. 14: Previous (left) and current (right) installation in the electricity room at Älvkarleby. Central left is the power meter PQube. Central middle is the communication box to receive reference solar cell (serial RS485 communication). Bottom right is the SolarEdge energy meter that communicates (sensors) to SolarEdge monitoring platform.

For the purpose of creating the shading of the arrays, a semi opaque fabric mesh for the direct shading experiment and a real pine tree for the obstruction shading experiment are the materials to be used. The fabric material chosen is a 100% polypropylene fleece fabric of dimensions 1.4 x 25 m, and it has a weight of 3.2 kg. This means that the cloth has a density of 0.091 kg/m^2. The pine tree is calculated to be 9.70 meters high to create shadow on the second row of solar panels for the time of the year when the experiment is performed. The calculations supporting the latter stated are shown in Appendix A.

Power quality monitoring of the two PV systems is done with the power monitor PQube 3e (Fig. 15). It has four three-phase load groups: Load of the laboratory, SolarEdge system, Fronius system and a battery located in a container one floor down which is charged from the main powerline. This product is a high precision meter and real-time sensor that also provides environmental sensing and external process measurements. It can connect directly to voltages up to 690 V, measure in real time and record 2 kHz ~ 150 kHz emissions of wave noise.

Fig. 15: Power quality meter PQube 3e AC Analyzer

In order to measure the I-V curves of the solar arrays, the photovoltaic tester MI 3109 Eurotest PV lite from Metrel® was facilitated (Fig. 16). This device performs all necessary tests required

on PV installations. The parameters needed for the I-V characteristic measurement are shown in Appendix B.

Fig. 16: I-V tracker MI 3109 Eurotest by Metrel

For this work the two PV systems were moved from original East oriented roof with tilt first row of 7 degrees and second of 10 degrees to a southernly orientation with 20 degrees tilt that is more typical for residential PV installations in Sweden. In the roof area ahead of the PV systems, the tree is mounted and secured for the test. A laboratory room equipped with the two inverters, the power meter and a computer serve to collect and handle the data.

The technical specifications and datasheets of the materials and the instruments described in this section are shown in Appendix D.

3.3. Procedure

The proposed methodology will investigate the performance of two types of PV systems: string configuration and individual module optimizers. Experiments focus on evaluating the energy production and the behavior under shaded conditions. Analysis will draw from fundamental engineering principals coupled with experimental data to create empirical models describing the behavior of the system. This process is carried out in the following steps, described in chronological order as they have been performed:

3.3.1. Comparison for unshaded conditions

Prior to the shading experiments, both systems are measured under unshaded conditions. This allows to normalize the results and it serves as a reference scenario for comparisons.

- **Comparison of East 10° and South 20° configuration**

Both systems were first facing East with a 7 to 10-degree tilt. The optimal configuration for the PV systems in central Sweden to work at their maximum performance occurs when they are South oriented at 42 degrees inclination. Additionally, most of residential rooftops are tilted 20-35 degrees. For these reasons the two systems were moved from their initial position to be South oriented with a 20-degree tilt. In this part the PV production of each system East-oriented is compared to the output achieved facing South to justify this decision.

- **Comparison of both PV systems for new configuration**

The complete system with the final configuration is shown in Fig. 17, where both systems can be appreciated, and the reference solar cell in between the two, at the bottom row.

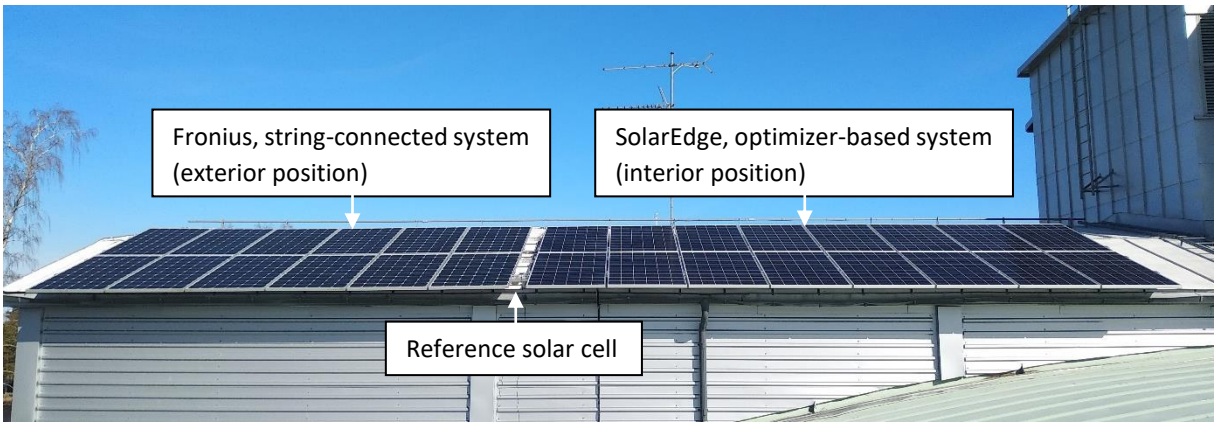

Fig. 17: Outlook of the systems and the reference solar cell for final configuration

Before the installation of the systems for this new orientation, the first aspect to be brought into contention is the position of each one of the systems, as well as the positive and negative factors that might affect. For this case, there were two placement options: interior and exterior position of the South-facing roof. All possibilities that may affect the project and the different experiments to be carried out must be considered. It should also be noted that the comparison carried out during the present study is between a string-connected system and a system with optimizers, from which improved results are expected with respect to the first one. Many aspects determine which location is most favorable for a PV system and care was taken to ensure that results were not biased by unfavorable position of the string-based system. The following situations have been observed, to conclude that the interior location is the most negatively affected by shading:

The interior position is affected by the adjacent wall: part of the SolarEdge system is shaded on the upper row of the array in the morning. Since this occurs in the morning, the shade generated is sharp and more severe. On the other hand, for the experiment with the tree, this system receives a more diffuse radiation since the shade from the tree occurs in the afternoon-evening, which leads to less production losses. Since this position is closer to the lower roof area underneath the systems, this causes reflection on the SolarEdge system, which is beneficial because it absorbs more overall radiation. However, the fact that this system is closer to the roof below, means that it is receiving less ventilation and therefore the temperature will rise, which causes a decrease in its production. Moreover, and regarding the tree experiment, the SolarEdge production is affected by the higher temperatures in the afternoon, which is when the system is shaded by the tree.

Taking all these facts into account, and bearing in mind which ones affect in a more severe manner to the systems, it is elucidated that the disadvantages of placing a system in the interior position outweigh the ones for the external location. It is thus clear that the Fronius, string-connected

system is under favorable conditions, so as to ensure the measured shading mitigation from optimizer-system is not an effect of the PV systems relative placement.

3.3.2. Shading test procedure with new orientation

To guarantee that both arrays are receiving the same amount of radiation under the same weather conditions, they must be placed side by side and with the same orientation and tilt, and the shading must be created simultaneously for the comparison to be accurate. Measurements must be taken on clear sky days and in the range of time when irradiance is higher to obtain the best outcome, i.e. right before and after the solar noon. Calculations detailing how the solar noon is obtained for these specific coordinates are shown in Appendix A.

- **Simulated snow coverage with fabric mesh**

This experiment aims to show the merits of the optimizer-based system under PSC. For this purpose, shading is applied with a translucent fabric mesh attached to the bottom row of both systems covering up to 60% of each module, as an emulation of snow cover (see Fig. 18).

The cloth selected in this experiment is a fleece fiber cloth with 0.09 kg/m^2 density. It is assumed to have an average of 50% of transmittance around midday, (as it can be seen in Fig. 2 from Appendix A) meaning that it allows 50% of the sunlight to pass through the fabric and reach the solar panels. However, it is very important to note that the amount of light that penetrates the material is not constant during the day, as it is heavily dependent on the angle of incidence. The transmittance of the cloth corresponds to a certain amount of snow, since the transmittance of snow coverage is heavily dependent on its layer thickness [30]. This is explained in detail the Discussion chapter. Calculations showing how the transmittance is obtained are found in Appendix A. The fabric mesh is set over the systems for 2 days, considering this time enough to collect the needed data for the analysis.

The total blocked irradiance over the systems is approximately 15% (50% of the system shaded with cloth covering 60% of the modules with a transmittance of around 50%).

Fig. 18: Systems with snow cover on bottom row

- **Tree shading**

With the aim to recreate a more realistic shading pattern a pine tree is placed in front of the arrays. This experiment has the objective of simulating the shade created by nearby trees on residential PV installations coming from neighboring properties or wooded areas. The length of the tree is calculated to create shade on the arrays until the completion of the experiment. This is calculated following the equations found in [31], resulting in a height of 9.70 meters, as it is demonstrated in Appendix A. The distance from the tree to the PV arrays is selected to be similar just over the minimum distance allowed for Swedish properties between the fence and the house construction, which is 4.5 meters. The tree is placed in the middle of the systems so that it creates shadow on both systems in the most analogous and comparable way. This decision is supported by the fact that since the arrays are south oriented, the tree shadow hovers in between the two systems at solar noon, which is when the irradiation is maximum. The shadow created by the tree is such that the Fronius system is shaded in the morning and the SolarEdge system is shaded in the afternoon. The final set up for this experiment is shown in Fig. 19.

Fig. 19: Perspective of the systems for the tree shading experiment

- **Characterization of I-V curves**

With the objective of gaining a better understanding of the PV systems behavior under PSC, the I-V characteristics and power graphs are obtained for both a stand-alone small panel with the fabric mesh and also for the full 60-cell module within the tree shading experiment for a single module of the same type as used in the SolarEdge system. The instrument utilized for this purpose is selected to use the testing standard IEC 60891, an international standard which gives procedures

for temperature and irradiance corrections to the measured I-V characteristics of crystalline silicon photovoltaic devices. The parameters needed for the test are show in Appendix B.

The I-V curves and power graphs measured on the small independent panel – SunModule sw50 poly RMA- are performed on a solar module for different shading patterns under the semi-opaque cloth. This PV panel consists of 2 circuits in series of 18 silicon cells, and 2 bypass diodes, one in parallel to each circuit. The datasheet is found in Appendix D. The scenarios contemplated are described in Table 1. The behavior observed for this module can be extrapolated to the main modules this study is focused on, as it is explained in the subsequent chapters.

Table 1: Shading case scenarios on stand-alone module

Case	Description
0	Unshaded
1	3 rows of cells shaded on 2 circuits: 12 cells, 6 each circuit (1/3 module shaded)
2	6 rows of cells shaded on 2 circuits: 24 cells, 12 each circuit (2/3 module shaded)
3	Entire module shaded: 36 cells
4	½ circuit shaded: 9 cells of 1 circuit
5	1 circuit shaded: 18 cells of 1 circuit
6	1 circuit 1 shaded and ½ circuit 2 shaded: 18+9 cells
7	Diagonal shading
8	1 rows of cells shaded on 2 circuits: 4 cells, 2 each circuit (1/9 module shaded)
9	1 cell shaded in 1 circuit
10	6 cells shaded in 1 circuit
11	1 cell in 1 circuit shaded with 100% opaque tape
12	1 cell in each circuit shaded with 100% opaque tape

The I-V curves measured are taken on the roof facilities where the two main systems – Fronius and SolarEdge – are installed, 20 degrees tilted and facing South. Measurements took place at solar noon on a clear sunny day, in order to measure under the best irradiance conditions. Images of the shading scenarios on the independent module are shown from Fig. 20 (a to l) to give the reader a more visual overview of the study.

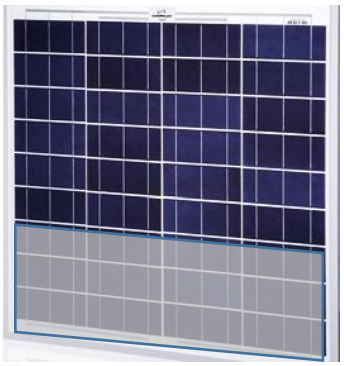

Fig. 20 a): Shading case 1

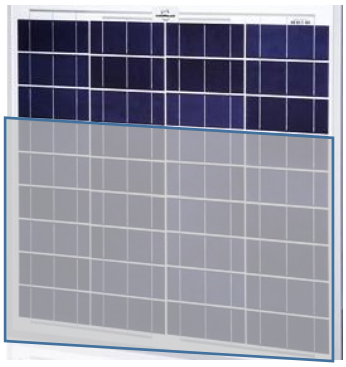

b): Shading case 2

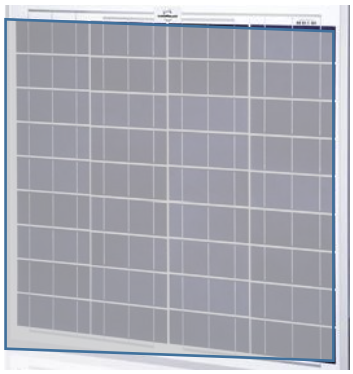

c): Shading case 3

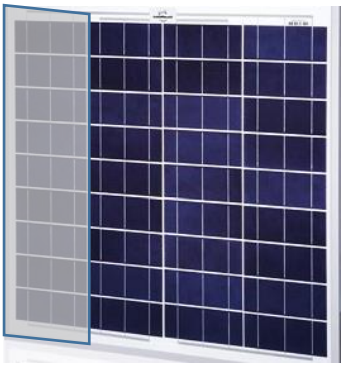

d): Shading case 4

e): Shading case 5

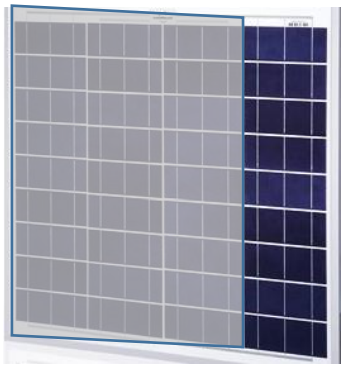

f): Shading case 6

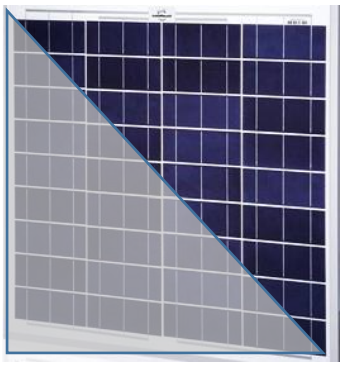

g): Shading case 7

h): Shading case 8

i): Shading case 9

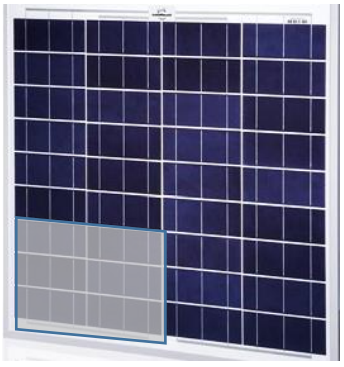

j): Shading case 10

k): Shading case 11

l): Shading case 12

Regarding the I-V characteristics within the tree shading experiment, they are performed on the bottom row of the system. The measurements are taken every half an hour, following the shade of the pine tree over the system. They correspond to the shade projected on each module of the system, as it is clarified in Table 2.

Table 2: I-V characteristic measurements for the tree shading experiment on single SolarEdge module

Measurement number	Time (hours)	Module number
0	Unshaded	
1	13:30	1.0.16
2	14:00	1.0.12
3	14:30	1.0.7
4	15:00	1.0.4
5	15:30	1.0.6
6	14:00	1.0.11

These measurements correspond to the following shading pattern, as seen from Fig. 21 (a to f):

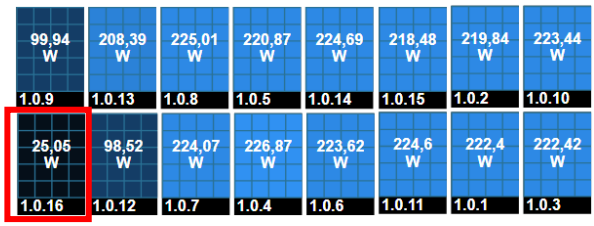

Fig. 21 a): Measurement 1

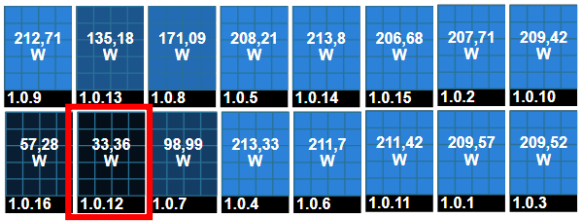

b): Measurement 2

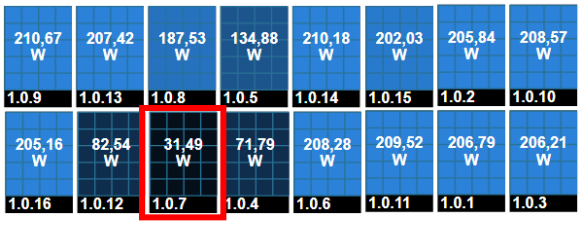

c): Measurement 3

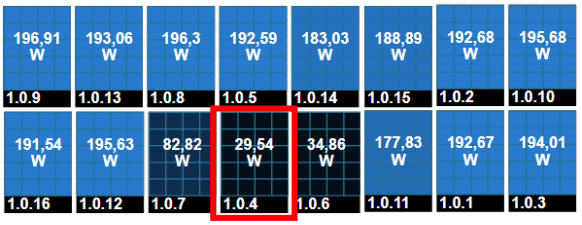

d): Measurement 4

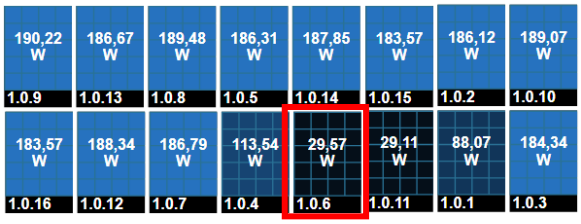

e): Measurement 5

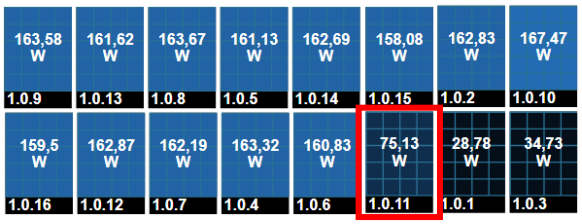

f): Measurement 6

3.3.3. Data analysis

The aim of data analysis is to characterize these configurations and to give this report the opportunity to serve as a helpful tool of reference for future residential PV installations. The energy production for the different shade scenarios and experiments was collected from the power quality meter PQube. In addition, the internal inverters measurements are used for comparing each systems production. The power quality meter was installed in the laboratory room after the systems were moved to their new location on the roof – 20° South-, ergo for the comparison of the production 10° East and 20° South, power values were extracted from the respective inverter monitoring interfaces of each one of the systems. On the other hand, for the snow cover and the tree shading experiments, energy production was taken from the power meter PQube.

Regarding the comparison of each system in reference to its ideal performance, the selection of this data has to look carefully at all the influential factors that might affect the production for each set of values, such as the irradiance and ambient temperature records. In view of this, the days for comparison will be as closest in time as possible, to minimize errors. In addition, the systems are compared one to the other. In order to make it possible, the production is normalized according to the maximum capacity of each system.

The results presented in this report show the normalized production of both systems. This is necessary to make pairwise comparisons, because the systems do not have the same size. The total electrical power is obtained from the PQube meter in Watts (W). Data is given for the time interval selected in the instrument and it corresponds to the total system production. It is normalized as follows:

$$Normalized\ production = \frac{Power\ (W)}{system} \cdot \frac{system}{N\ modules} \cdot \frac{module}{Max.Power\ (W\ peak)} \qquad (8)$$

As for the shading experiment with the cloth that simulates snow cover, the fabric mesh is set over the systems for 2 days, considering this time enough to collect the needed data for the analysis. One of these days is picked for the comparison with a sunny day when the production of the systems is expected to be maximum.

Concerning the study of the yield of the arrays for the tree shading experiment, several factors must be taken into consideration. Firstly, and with the aim of doing the analysis in the most accurate way as possible, the comparison looks at the hours around solar noon since it is when insolation reaches its highest levels. Ideally, production values should be compared at the exact same time, however since the tree performs shade on the systems at different time of the day this cannot be possible: the Fronius system is shaded in the morning whereas the SolarEdge system is shaded in the afternoon. The daily irradiation follows a symmetrical trend with respect to the solar noon, and the tree shadow lies right in the middle of the systems at this time. Hence, it is acceptable to compare the production between both systems because the irradiance levels are equivalent.

Note that the PV systems are not facing the exact South, but are slightly deviated to the West (7 degrees azimuth). This means that the shadow is not perpendicular and in the middle of the systems at solar noon but 28 minutes after this time. The comparison is therefore made by setting this time as the reference or zero time from which the system′s production is studied. In the Appendix A this exact time is calculated, given the solar angles equations that appear in [31].

3.4. Ethical considerations

The proposed research is merely a study of the performance of residential PV systems and does not intend to harm nor injure any person in the course of the experiment, hence no ethical considerations are worth mentioning.

4. Results

Practical results presented thereon show the merits of optimizer systems under shading conditions. Based on previous studies and investigations carried out by experts in the field it is known that the use of micro-inverters or optimizers will improve the system performance in any case [17], [32], which is supported in the present study.

The production has been normalized per module, since two systems of different size cannot be compared otherwise (16 and 12 modules). Note that Fronius and SolarEdge modules have different maximum power capacities. The Fronius system´s modules are rated at 275 W peak while the SolarEdge modules are rated at 270 W peak. However, it has been considered that the maximum power capacity of both systems is 270 W peak. This decision is supported by the fact that the Fronius system is 2 years older and, according to the manufacturer, it would have lost 2% of its peak power due to degradation, which results in 270 W peak.

4.1. Unshaded conditions

The first data analyzed in this study belongs to the production of the systems with the original configuration, which is East oriented and with a 10-degree tilt. This production is compared with the final configuration: South oriented and a 20-degree tilt. Data from the inverters internal measurement is used here. It can be observed that both SolarEdge and Fronius systems have an increased output for the new set up for the new configuration.

In Fig. 22 it is shown the normalized production of SolarEdge system for both configurations. The new disposition presents a gain of 30% with respect to the previous one. Similarly, Fig. 23 shows the normalized production of Fronius system, with a 36% gain of the new set up in reference to the initial one.

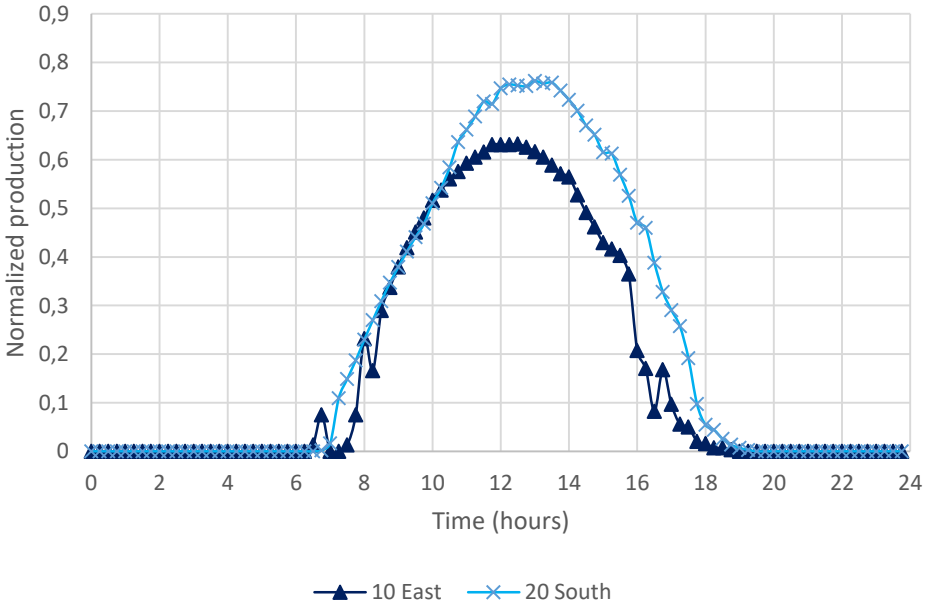

Fig. 22: Normalized production SolarEdge system East and South oriented

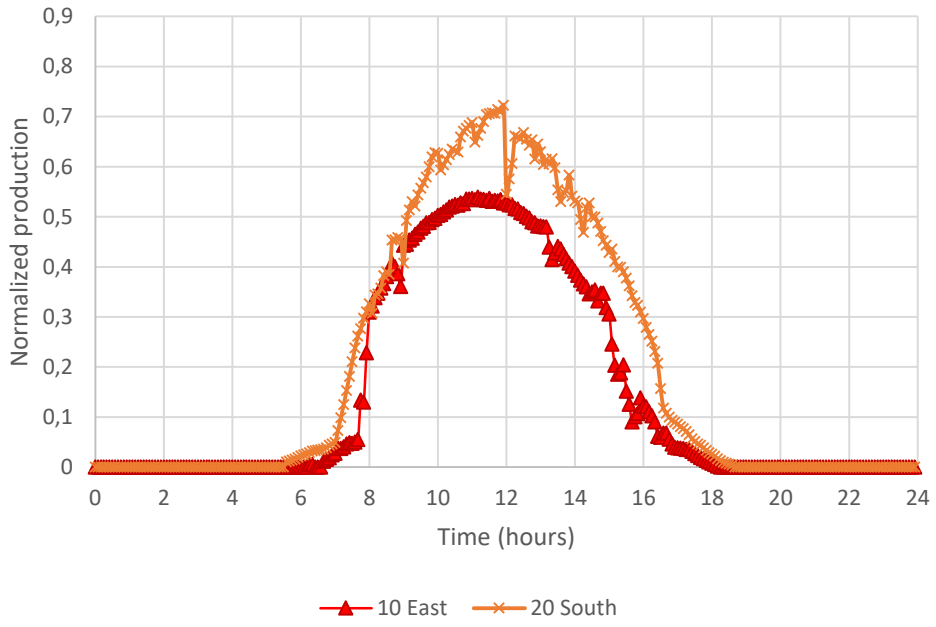

Fig. 23: Normalized production Fronius system East and South oriented

Henceforward, the information presented belongs to the systems facing the South for the months April and May. Data is measured with the power meter PQube from now on. It is observed that the solar noon is shifted one hour due to light saving (13:00 instead of 12:00, local time).

The following plot (Fig. 24) shows the power delivered by each system per square meter and the daily irradiance for a sunny day in April. It can be observed that for unshaded conditions both systems perform equally. If anything, SolarEdge system has a slightly higher production which can be either because the systems modules are newer and have not experienced the same degradation, or because the SolarEdge inverter has a higher efficiency (97.5% SolarEdge versus 96.2% Fronius, values given by the inverters' manufacturers in their respective datasheets).

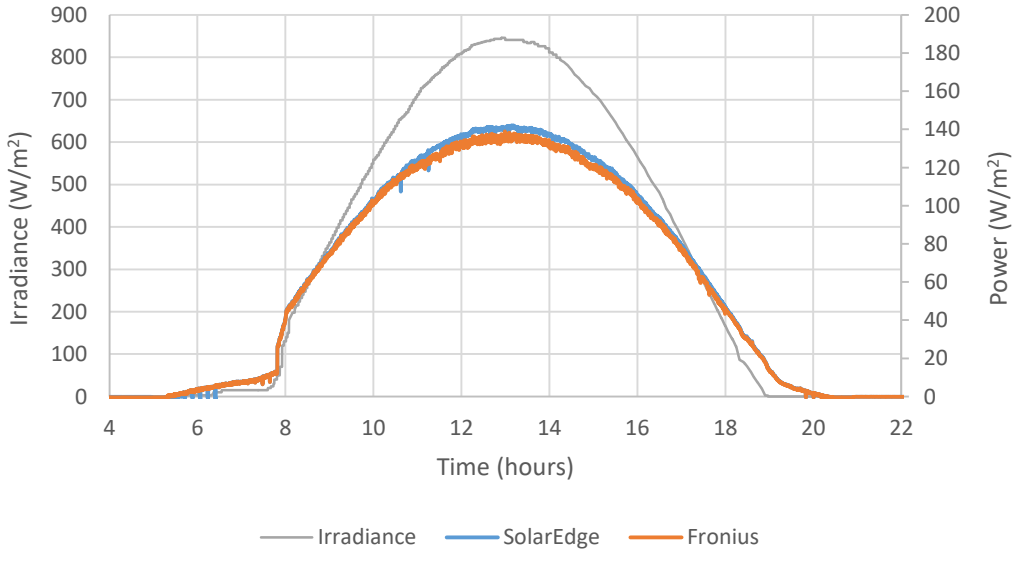

Fig. 24: Daily irradiance and production of both systems for a sunny day

This graph is also used to calculate the systems efficiency, as it is seen in Fig. 25. Calculations are given in Appendix A. The efficiency is mostly constant except for the early morning and evening hours, which can be attributed to the fact that there is more scattered radiation. At this time, the systems will still produce even if the direct radiation is at a lower level. Moreover, the reference solar cell has strong angular dependency and might be affected by reflectance and/or shading, measuring lower irradiance than there actually is. Fig. 25 shows a zoomed graph for the central hours of the day, where it can be clearly seen that the efficiency of both systems is 16.5%. This experimental finding corresponds to the efficiency given by the manufacturers, as it can be checked in the datasheets in Appendix D. The lower values around the central hours are due to the higher temperature of the modules.

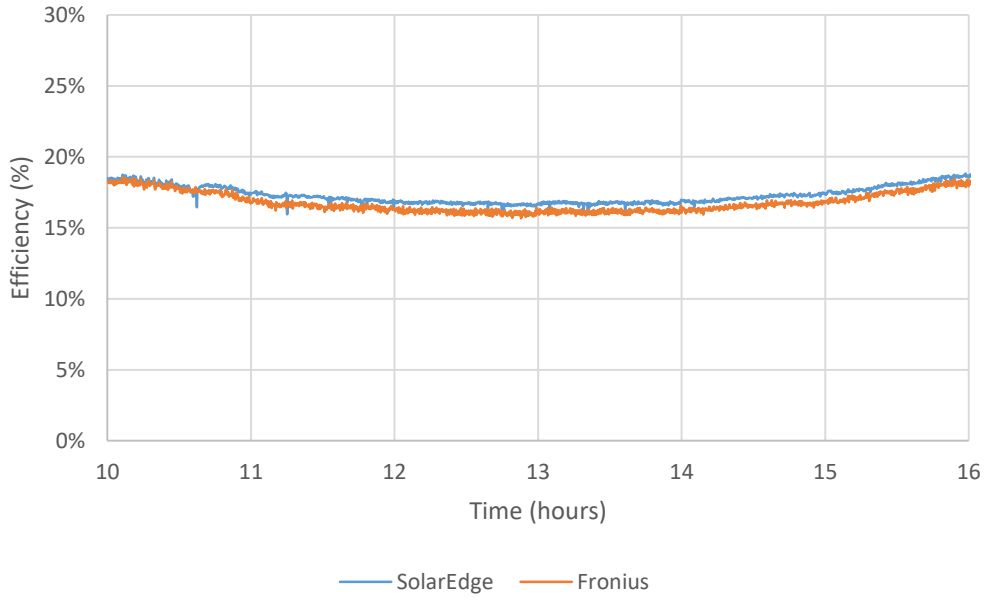

Fig. 25: Closer view of the Efficiency of both systems for central hours

4.2. Simulated snow cover with fabric mesh

Here in Fig. 26 it is presented the normalized production of both systems under good light conditions, where both systems have identical performance. Fronius systems has minor shortfall around 18:00 as it can be observed in Fig. 26, which is due to the shade from the trees on the riverside. SolarEdge system is partly shaded in the morning due to the adjacent wall. The SolarEdge production appears to overtake the Fronius system production after 10:30, which is when the shade from adjacent wall is no longer affecting the system. However, it cannot be appreciated in the graphs herein presented, since the production during this time has been compensated according to the maximum yield of the unshaded modules. In Fig. 27 it is shown the production of SolarEdge system in the morning, where the shaded modules due to the adjacent wall are yielding less power than the rest, working only with diffuse and reflected radiation. To compensate this power loss, it has been assumed that all the modules are unshaded as if there was no wall shadowing the upper row.

In any case, and for all the experiments, the production of the systems is studied around the central hours of the day, i.e. three hours before and after solar noon, to avoid unnecessary sources of error and because the irradiance is at its maximum daily levels.

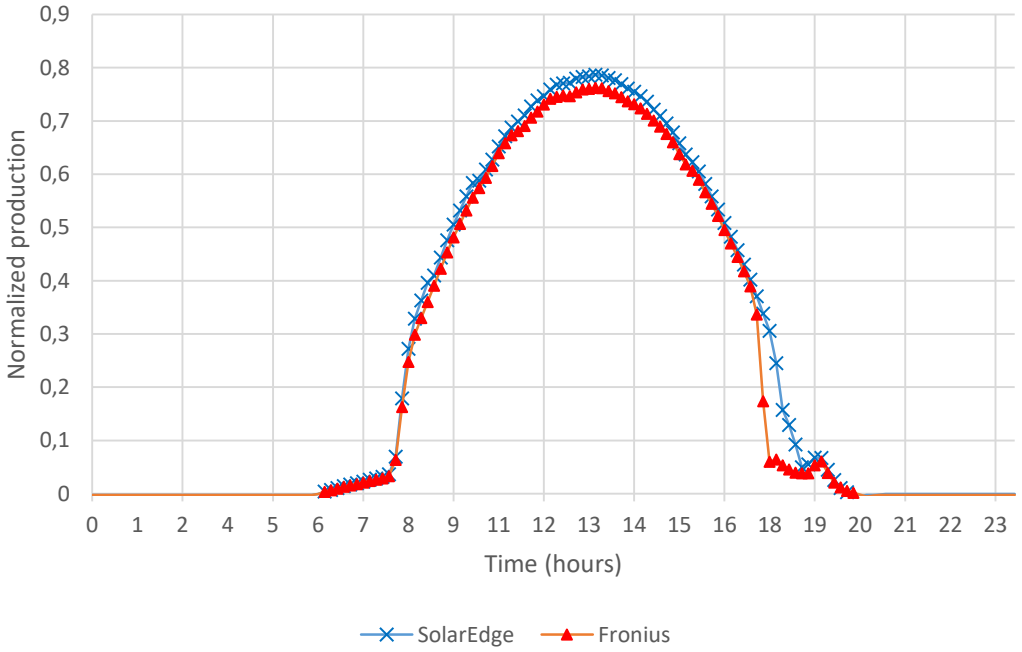

Fig. 26: Normalized production of both systems for unshaded conditions

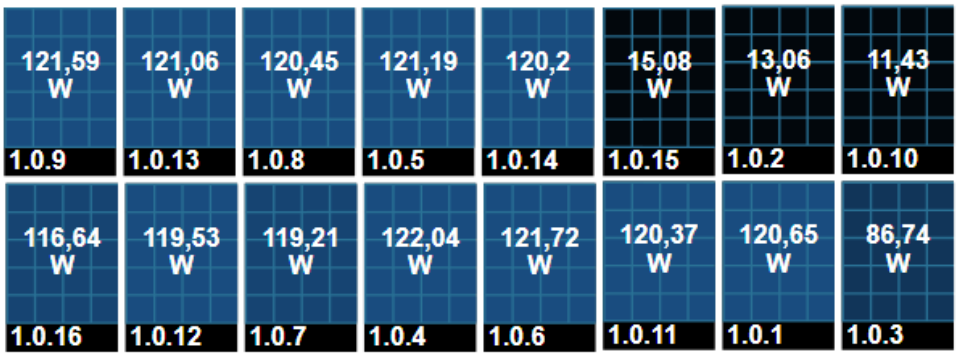

Fig. 27: SolarEdge system at 9:00 in the morning, upper row partly shaded due to adjacent wall

Results from the direct shading experiment with the fabric mesh are positive for the SolarEdge system. SolarEdge system production loss due to the simulated snow cover is 29%, whereas Fronius losses are 50% (see Fig. 28). When both systems are compared between them, the shading losses are decreased by 18% with optimizer SolarEdge system in comparison to the string-based Fronius system (see Fig. 29). As stated before, only the production between 10:30 and 16:30 is utilized for comparison. The SolarEdge system is observed to present no gain outside this time range (before 10 and after 17 hours). This is further analyzed in the Discussion chapter.

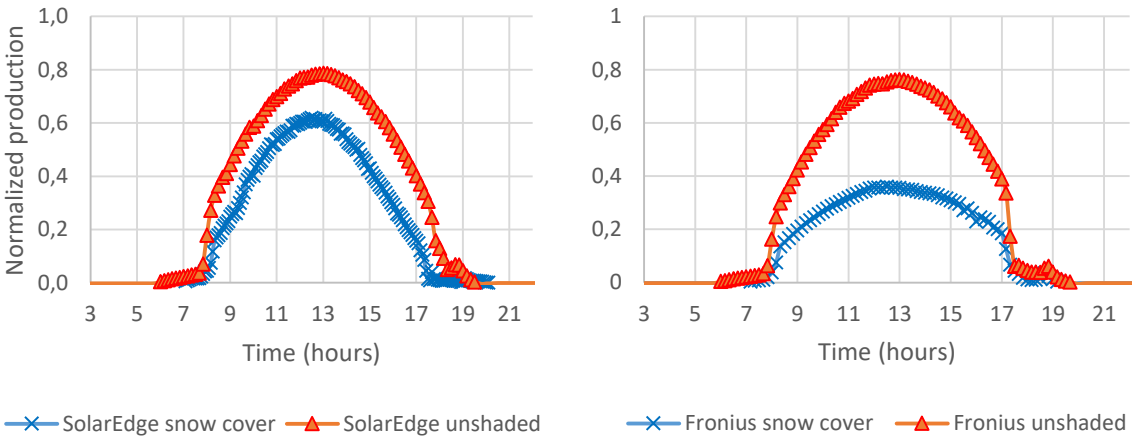

Fig. 28: SolarEdge and Fronius relative energy losses due to simulated snow cover

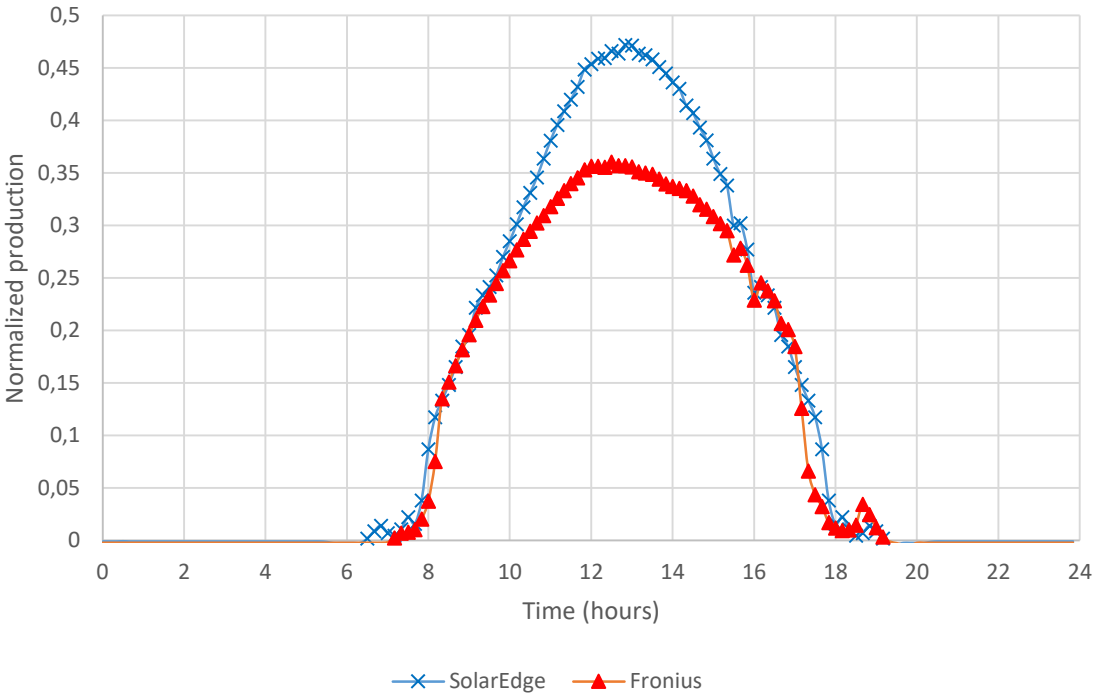

Fig. 29: Normalized production of both systems under fabric mesh shading

4.3. Tree shading

The experiment with obstruction shading with a pine tree rendered positive results for the SolarEdge system. The losses due to shading were shown to be reduced from 17% to 13% with the optimizer-based system. Fig. 30 and Fig. 31 show the normalized production of each one of the systems in comparison to their unshaded condition.

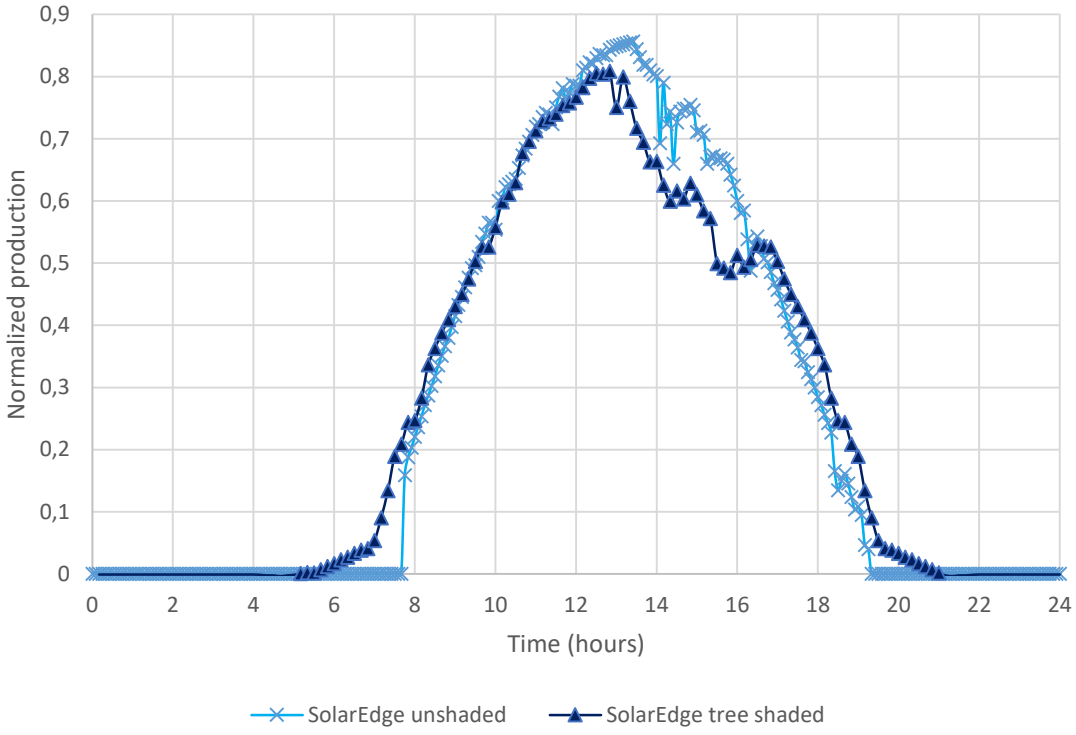

Fig. 30: Normalized SolarEdge production under tree shading compared to unshaded system

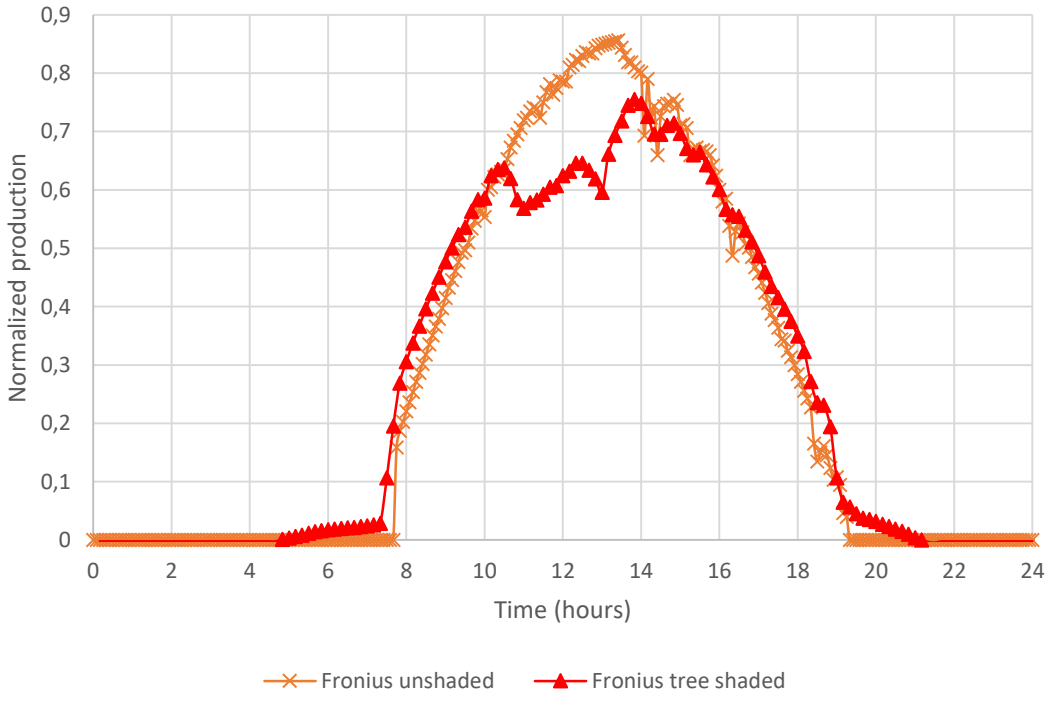

Fig. 31: Normalized Fronius production under tree shading compared to unshaded system

Fig. 32 displays 5% more power losses for the Fronius system in comparison to the SolarEdge energy production.

The shading pattern that has been explained in the Method chapter can be visualized below (Fig. 32). The Fronius system undergoes the tree shading losses in the morning, starting at 10:30, and then the SolarEdge system is shaded in the afternoon until 16:30 hours. The vertical line drawn on the graph represents the moment the tree shadow is perpendicular and right in the middle of the two systems, which occurs at 13:15. As it can be perceived, the Fronius system starts rising at this time as the SolarEdge system becomes shaded.

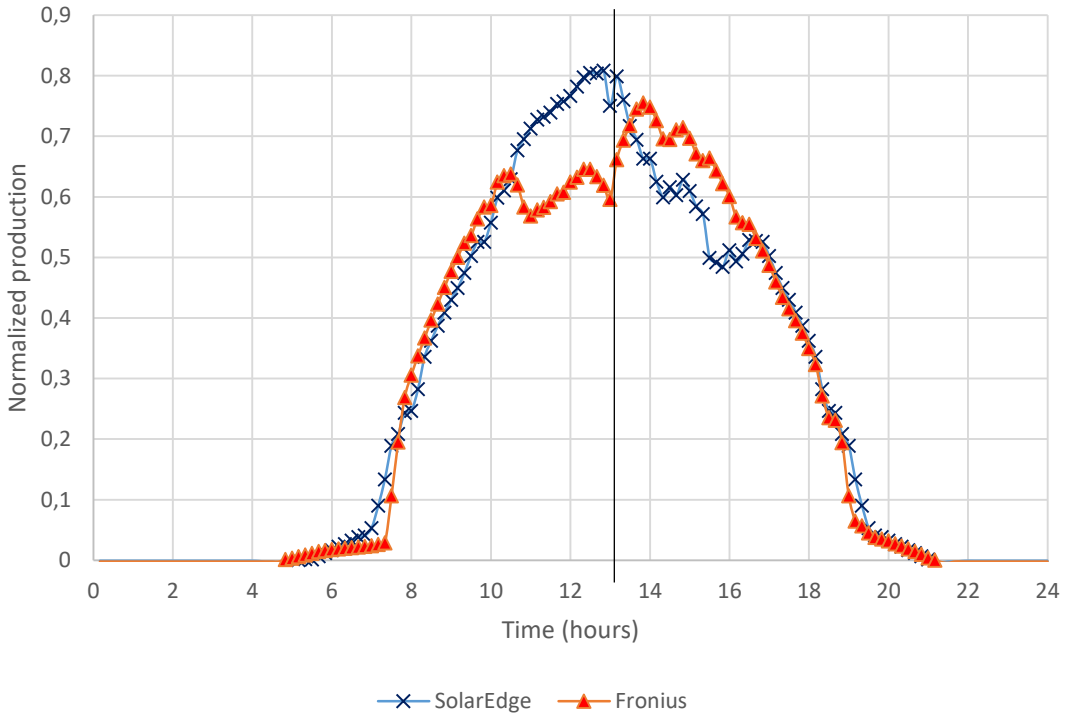

Fig. 32: Normalized production of both systems under the tree shading

Additionally, and as complementary material of the experiment, the I-V characteristic and power graphs are obtained on a single module of the SolarEdge system, following the tree shade projected on the modules of the system. The information regarding the measurements and the shading pattern is detailed in the Method chapter (see Fig. 21), and the experimental visual results (I-V curves) are found in Appendix B. As seen below, Table 3 gathers the key values of the experimental graphs obtained, and the real power measured with the power meter PQube:

Table 3: I-V and P-V curve measured parameters of the tree shading experiment, and MPP from power meter

Measurement	$V_{oc}(V)$	$I_{sc}(A)$	$V_{mpp}(V)$	$I_{mpp}(A)$	$P_{mpp}(W)$ *I – V measured*	$P_{mpp}(W)$ *power meter*
1	32.8	1.59	30.7	0.94	29	25
2	33.2	1.34	30.5	1.12	34	33
3	34.2	1.01	32.3	0.88	28	32
4	34.1	1.03	31.2	0.91	29	29.5
5	34.5	0.98	33.2	0.81	27	29.6
6	35.1	2.06	33.9	1.10	37	75

If the MPP measured results are compared, they are observed to be very similar. The only value that differs from reality is Measurement 6, but in general it can be said that the results are rather consistent. The I-V curves obtained are coherent with the theory and the shading observed on the modules. However, these results can act as data for verification of theoretically obtained I-V curves, as it is exposed in section 6.2: Outlook and future recommendations.

4.4. Effects of shading on stand-alone module

As it has been described in the Method chapter, various shading patterns with the semi-transparent cloth are applied on a stand-alone module. The current-voltage and power graphs are displayed in Appendix C, which correspond to the shading scenarios Case 0 to Case 12, detailed in Table 1.

The deductions and judgement drawn from these plots are reviewed in the following chapters, Discussion and Conclusions.

5. Discussion

Critical evaluation of the findings presented in the Results is given in this chapter, and reference to the aims and hypothesis stated at the beginning. The validity of the approach and method followed to conduct the experiments is also discussed, as well as uncertainties related to the instruments employed.

Firstly, and in order to work with a common reference to both systems and to eliminate errors the data has been measured with the same power meter: the power monitor PQube 3e. The instrument interface allows the user to select the desired time resolution to collect the data. Although daily power values were the required data aimed to analyze, there were selected complementary interrelated parameters such as the current, voltage, harmonics, energy, etc. to gain a broader understanding of the variations and the values obtained. They were also very helpful in situations of mismatching data or unforeseen events that affected the measured power.

However, for unshaded conditions comparison (10° East vs 20° South), energy production data was taken from the inverters' measurement interfaces. This could have introduced certain discordance, because each brand has different software implemented to measure and display the power their systems are delivering. Nevertheless, we were aware of this is factor of uncertainty and therefore the systems were not compared one to the other, but the relative production of each system from its previous orientation to the new one was examined instead. In such way it is valid to compare the data since there is a local reference for each system.

5.1. Comparison East 10° vs South 20° placement

Regarding the results from the comparison of the initial disposition of the systems (10° East) with the new one (20° South), it is observed that the PV systems present great increase in their energy production with the new configuration. Both systems undergo similar gain: 36% for Fronius and 30% for SolarEdge. The reason for the slightly larger gain of Fronius could not be delivered. There might be some disparities due to the days selected for the analysis, although the irradiance corresponding to the data is equivalent. These results corroborate the hypothesis that the optimal orientation of a residential PV system is towards South in the Northern hemisphere. It is evident that this orientation would result in a higher output since it is more exposed to sunlight and it is perpendicularly oriented to the sun path.

5.2. Simulated snow cover with fabric mesh

The experiment with the semi-transparent cloth compares two days of production: a day with the cloth over the modules to a sunny, unshaded day. For the comparison to be as accurate as possible, the external conditions such as the irradiance during the day and the temperature have to be similar. The days this experiment was conducted were partly cloudy, whereas the sunny day picked for the comparison was clear and sunny. Hence, the production had to be normalized according to the irradiance of the two different days so that both scenarios were comparable. This was done by setting the sunny day as the reference irradiance scenario, and correcting the power

data of the shaded day given by the power meter, to match the irradiance of the day set as a reference. It is basically a directly proportional method to scale the production as a function of the irradiance.

The fabric mesh utilized for this experiment is meant to emulate snow cover on the PV modules during the winter season. The cloth transmittance is assumed to be 50%, which is comparable to 1 cm of snow, according to Fig. 33 (b), found in [30]. The snow transmittance depends on the irradiance wavelength, which varies during the day due to different irradiance levels. Visible sunlight belongs to the photosynthetically active radiation, which is the radiation capable of creating the photovoltaic effect on solar cells. In this zone of the spectrum, snow produces high light scattering [33], reflecting most of the incident sunlight and transmitting little. Unlike reflected radiation, transmitted light is very dependent on the spectral wavelength. The study [30] investigated snow transmittance as a function of the layer thickness and the radiation wavelength, from where Fig. 33 (b) has been found useful on this matter. The cloth transmittance also varies during the day, as it can be verified in the Appendix A and shown in Fig. 33 (a). However, in practice and for this experiment, the transmittance is not dependent on the wavelength for the values obtained, since they are not below 0.1. Note that the cloth transmittance calculation might not be accurate enough since it should have been determined using the data from the reference solar cell instead of the systems production.

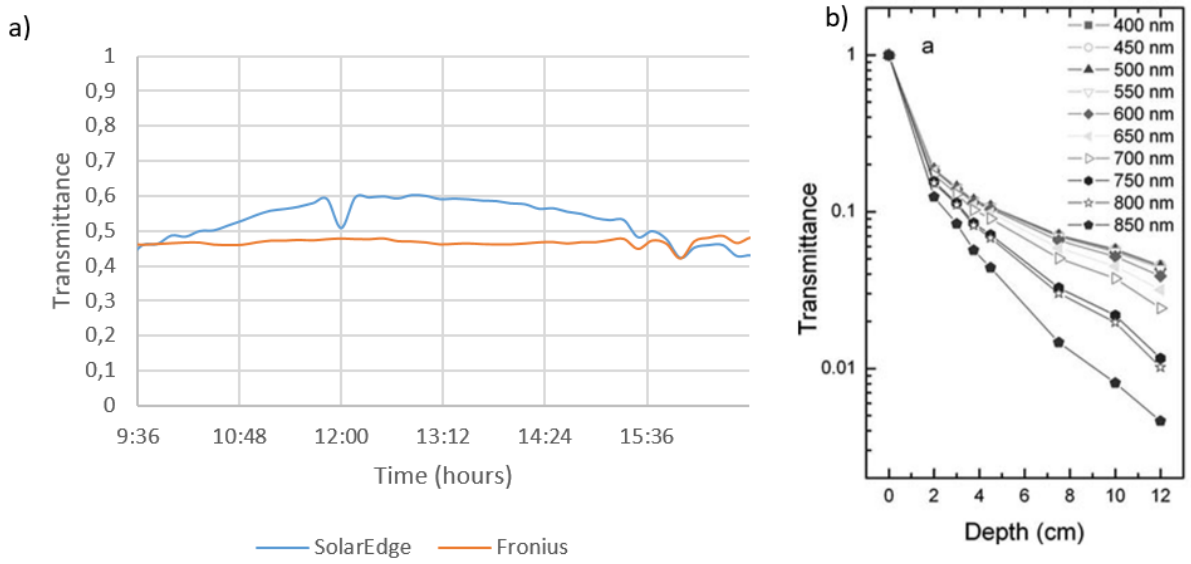

Fig. 33: Experimentally obtained transmittance of the cloth used in the experiment (a) and transmittance of snow as a function of the layer thickness and irradiance wavelength [30] (b)

Results obtained in this experiment showed that SolarEdge system performed better than Fronius for the central hours of the day, whereas both systems appear to have similar normalized production in the morning and evening. The SolarEdge system is yielding the output of the 8 unshaded modules and also the contribution of the 8 shaded ones up to 50% (50% transmittance of the cloth). On the contrary, the Fronius system has half of the array bypassed during central hours, harvesting half of the production in comparison to a sunny day, due to the fact that the

bypass diodes go into effect. The similar behavior of the systems outside the time range object of study could be explained because the transmittance of the cloth decreases drastically in the morning and evening hours. This is due to the lower angle of incidence of sunlight radiation, and because there is less irradiance. Therefore, the sunlight reaching the modules is not enough and the contribution of unshaded SolarEdge modules is very low, leaving no opportunity for the optimizers to outperform the string-connected system. Even so, the experimental results verify the gains of the optimizer-based system at large.

5.3. Tree shading

As for the tree shading experiment, a 9.70 m high pine tree is placed in front of the arrays, centered in between the two systems at a perpendicular distance of 5 m. The shadow created by the tree is such that the Fronius system is shaded in the morning and the SolarEdge system is shaded in the afternoon. The shade is perpendicular and in the middle of the two systems at 13:15 hours. This is because the systems are not facing the exact South, they have an azimuth of 7° towards West. If they were looking towards the exact South, the tree shadow would lie in between the systems at the exact solar noon (12:47), calculated in Appendix A. But because the systems have an azimuth, this occurs 28 minutes after this time, i.e. at 13:15 hours. Thereby, the comparison of the shading losses is made 3 hours before and after the time that the tree shade is perpendicular and in the middle of the two systems (13:15), that is, from 10:15 to 16:15 hours.

The shaded production is compared to the relative unshaded of each system to know their absolute power losses. Afterwards, the production is compared between systems to obtain the relative shading losses.

The shaded energy production data is extracted from the power meter PQube. The unshaded production can be obtained in two different ways: selecting a day before the tree was set up and taking data from the power meter PQube, or taking data from the reference solar cell the very same day that the shaded production is analyzed. In order to avoid errors due to different irradiance and temperature levels between days, the unshaded production is obtained with the reference solar cell.

The reference solar cell is located in between the two systems and it is measuring the irradiance continuously. The only time it is shadowed is when the tree shading is perpendicular to it (between 12:45 to 13:45 hours). With the aim of having the complete unshaded data, those values are extrapolated using data from sunny days before the tree was placed with similar radiation patterns and then the irradiance for the entire day was obtained. Afterwards, this irradiance was converted into the production of each system using the efficiency previously calculated for both systems, as shown in Equation 8:

$$Total\ system\ production\ (W) = Total\ system\ Area\ (m^2) \cdot \eta \cdot Irradiance\ (W/m^2) \qquad (9)$$

The SolarEdge system presents better results than the Fronius system for this experiment as well, in this case under partial shading conditions and a flickering pattern. As the Sun moves throughout the day, so the shadow projected passes along both systems. This is a more realistic shadow than the experiment where a cloth was applied and fixed to half of the modules, the tree shade is more diffuse and variable, as it is the case for most of the shade scenarios for residential PV installations. The use of optimizers is hence justified by the increased production over the string system.

Concerning the I-V curves obtained, it can be observed in Table 3 that the MPPs measured correspond to the real values, except for the last one. This is attributed to the lack of accuracy caused by the movement of the tree shade and the positioning of the module itself. Although these results verify the theory, their evaluation is out of the objective of this thesis. Nevertheless, they serve as verification of theoretical I-V calculation model developed at Vattenfall R&D.

5.4. Effects of shading on stand-alone module

The I-V characteristics and their respective power graphs obtained for the small stand-alone module brought some highlights as well, that can be applied for the study of the systems behavior under the simulated snow cover and for a better understanding of how bypass diodes work under PSC. All the I-V curves obtained are observed to change as the theory predicts.

Firstly, there has to be a high driving current to activate the bypass diodes in a shaded module, coming either from other unshaded modules or from the illuminated cells in the shaded module itself. A difference of 20% between the high current over lighted cells and the low current through shaded cells can be sufficient to activate the bypass diode of the circuit in the submodule.

The operating point of a module without optimizer is selected by the highest current, which is the one circulating over the unshaded circuit – although it does not entail the highest MPP. On the other hand, a module with optimizer works at the highest MPP.

It was concluded that the bypass diodes are not activated in any case till one single cell is 100% shaded (Case 11). In this scenario, the shaded circuit is bypassed, and only the unshaded circuit is working. For Case 12, consequently, 100% shading of one cell in each circuit means the open circuit of the entire module, giving no output.

For the rest of the cases, the semi-transparent fabric with approximately 50% transmittance is used. Blocking radiation partially on one single cell in once circuit (Case 23) gives almost the same I-V curve than if the entire circuit is shaded (Case 19), because the current is limited to the cell giving the least current. The operating point of these cases will depend on if the module has optimizer. In Case 8, 1, 2 and 3 the two circuits of the module are shaded progressively (11%, 33%, 66% and 100%). It is observed that regardless of the area that was covered, they all present the same I-V curve shape and very similar power losses. The MPP of these cases is not dependent on whether the module has optimizer or not.

When a shaded module is connected in series with other unshaded PV panels, its MPP is dependent on the incoming current from the unshaded modules. The bypass diode(s) is then

activated, and it will bypass the circuit(s) giving less current in the shaded module. If there is only one shaded circuit in one module, an optimizer-based system will activate the corresponding bypass diode and the module will give half of its production while the rest work at their MPP. For a string connected system, the entire module is bypassed and gives no power, while the rest work at their MPP. If, on the other hand, all circuits are shaded to a certain extent – as it is the case of the experiment with the semi-transparent cloth-, the current through the entire module is lowered. The optimizer-based system will work at this low operating power point for the shaded module and at the MPP for the illuminated modules. Conversely, a standard string system will bypass the entire shaded module and it will only deliver power from the unshaded modules.

This explains the functioning of optimizers and the reason why they are beneficial under PSC.

6. Conclusions

This study assesses the shading impact on different types of residential PV systems and shows the decrease in losses from partial shading conditions with power optimizers. It aspires to help PV owners select power inverters that maximize the annual energy produced.

6.1. Study results

Under unshaded conditions or for complete shade over all modules, both systems present the same I-V curve and the difference will lie on the MPPT technique implemented in their corresponding inverters, their efficiencies, temperature, etc. Hence under unshaded conditions optimizers per se will not result in a gain in PV systems energy output.

Optimizers become an advantage in case of partial shading conditions. Under this condition, optimizers work with maximum power, whereas the string connected system without optimizers work with maximum current over a PV module.

SolarEdge optimizers reduce shading power losses from 50% to 29% in comparison to a standard string system when simulated snow coverage is applied blocking 15% of the irradiance received. Shading losses are decreased by 18% with optimizer-based system.

The optimizers yield full production of the unshaded modules in addition to part of the production of the shaded modules, whereas the string connected system harvests only for the unshaded modules because the shaded ones are bypassed. Thus, it is concluded that optimizers are doing highest improvement when there is small shade over all the circuits of a series connected module.

For tree shading, SolarEdge system has a higher increased production in comparison to the Fronius system. Results show that SolarEdge system decreased tree shading losses from 17% in string-based system to 13% with optimizer-based system. Fronius system results in 5% more power losses in comparison to the SolarEdge energy production.

Overall, the use of optimizers under partial shading conditions has always proven to be beneficial in all the conducted experiments. The merit of an installation with optimizers will nonetheless depend on their additional cost and on their lifetime. However, this subject is out of the scope of the work herein presented.

6.2. Outlook and future recommendations

Recommendable future development of this work is given in this section to assess the study of optimizer-based systems under shading conditions.

Regarding the validity and accuracy of the findings presented, a standardized shading test procedure such as the one of the NREL – presented in the literature review section of this report - could be strictly followed. The calculation of the material used for the experiment with the semi-translucent mesh could have been done by means of using the data from the reference solar cell for more accuracy.

Concerning the tree shading experiment, a configuration with two trees – one for each PV array - could be used to observe the shading simultaneously on the two PV systems. Also, the results

obtained with the real tree employed in this experiment could be compared to artificially created shade emulating this same scenario, to compare which methodology is better related to real scenarios on residential PV installations.

Improvement in the method of the tree shading experiment would include a video camera placed on the roof where the systems are installed to keep track of the shading pattern and to record information. This way the data obtained with the power meter could be compared to these graphic data records in case external events or factors affect the systems production.

It would be interesting the study of battery energy storage with PV systems. The utilization of backup power would be useful for cloudy weather days and would lead to extra capacity. The behavior of PV systems under shading conditions when they are linked to energy storage could be object of analysis, as many households might find it an attractive solution.

In this project, time was scarce to make a comparison of the experimental results to theoretical data and to develop complementary software to simulate the systems behavior under the scenarios object of study. This could follow up the present investigation and would be a powerful tool to reproduce different shading patterns and scenarios and their impact on PV installations in a faster way, which would represent a breakthrough in the study of the shading effect and would spur the potential solutions to tackle it. Making reference to the experimentally obtained I-V curves under tree shading on a JinkoSolar module, their evaluation is out of the scope of this work. The results presented in Table 3 are intended to serve as verification of theoretical I-V calculation model developed at Vattenfall R&D.

6.3. Perspectives

Modern society is facing an energy problem, meaning that the energy demand is continuously growing, the population is increasing exponentially, and the resources are limited. The problem is that the current energy infrastructure is strongly dependent on fossil fuels, and it would take much effort to move towards renewable energies and build up or restructure the current situation. The main barriers are that it would require huge investments and a major change of attitude needed in society as a whole. Moreover, the current installed power of renewable energies cannot cover the world energy demand. Any measures that would help to increase the efficiency of these technologies would be useful to enhance the prospects of the renewable energies industry.

The use of power optimizers in PV systems has proven to decrease the energy production losses and therefore to increase the overall systems efficiency. Viewed from a broader perspective, and especially regarding energy systems at large, this study is an example of the many actions that can be taken towards helping the electrical network being more efficient and to improve the ever-growing use of solar technology as a source of energy.

References

[1] M. F. Acevedo, *Introduction to Renewable Power Systems and the Environment with R*. .

[2] O. Edenhofer *et al.*, *Climate Change 2014 Mitigation of Climate Change Working Group III Contribution to the Fifth Assessment Report of the Intergovernmental Panel on Climate Change Edited by*. 2014.

[3] Tomas Kåberger, "Progress of renewable electricity replacing fossil fuels."

[4] S. Silvestre, A. Boronat, and A. Chouder, "Study of bypass diodes configuration on PV modules," *Appl. Energy*, vol. 86, no. 9, pp. 1632–1640, 2009.

[5] International Energy Agency, "IEA-PVPS-Task1-Snapshot 2019 Report." [Online]. Available: https://www.iea.org. [Accessed: 19-May-2018].

[6] J. U. Tsao, N. Lewis, and G. Crabtree Argonne, "Solar FAQs."

[7] A. R. Jordehi, "Maximum power point tracking in photovoltaic (PV) systems: A review of different approaches," *Renew. Sustain. Energy Rev.*, vol. 65, pp. 1127–1138, 2016.

[8] Swedish Tax Agency, "mikroproduktionavfornybarelprivatbostad" [Microproduction of renewable electricity - private residence]. [Online]. Available: https://www.skatteverket.se. [Accessed: 15-March-2018].

[9] IEA PVPS, "2016 Snapshot of global photovoltaic markets," *Iea Pvps T1-292016*, no. April, pp. 1–16, 2017.

[10] S. Killinger *et al.*, "On the search for representative characteristics of PV systems: Data collection and analysis of PV system azimuth, tilt, capacity, yield and shading," *Sol. Energy*, vol. 173, no. April, pp. 1087–1106, 2018.

[11] R. Melicio, J. Figueiredo, L. Fialho, V. M. F. Mendes, and M. Collares-Pereira, "Effect of Shading on Series Solar Modules: Simulation and Experimental Results," *Procedia Technol.*, vol. 17, pp. 295–302, 2014.

[12] Y.-M. Saint-Drenan, "A Probabilistic Approach to the Estimation of Regional Photovoltaic Power Generation using Meteorological Data Application of the Approach to the German Case," no. August, 2015.

[13] A. Woyte, J. Nijs, and R. Belmans, "P artial shadowing of photovoltaic arrays with different system configurations: literature review and field test results," *Sol. Energy*, vol. 74, pp. 217–233, 2003.

[14] I. Pf, "Instruction Manual For The SolarPathfinder Unit ™," no. 931, 2016.

[15] P. Srinivasa Rao, G. Saravana Ilango, and C. Nagamani, "Maximum Power from PV Arrays Using a Fixed Configuration Under Different Shading Conditions," *IEEE J. Photovoltaics*, vol. 4, no. 2, pp. 679–686, Mar. 2014.

[16] C. Tubniyom, W. Jaideaw, R. Chatthaworn, A. Suksri, and T. Wongwuttanasatian, "Effect of partial shading patterns and degrees of shading on Total Cross-Tied (TCT) photovoltaic array configuration," *Energy Procedia*, vol. 153, pp. 35–41, 2018.

[17] SolarEdge Technologies Inc., "Performance of PV Topologies under Shaded Conditions,"

no. July, pp. 1–5, 2013.

[18] T. Dierauf *et al.*, "Weather-Corrected Performance Ratio Jose Luis Becerra Cruz Weather-Corrected Performance Ratio," no. April, 2013.

[19] L. El Chaar, L. A, and N. El Zein, "Review of photovoltaic technologies," *Renew. Sustain. Energy Rev.*, vol. 15, no. 5, pp. 2165–2175, 2011.

[20] A. Ferreira *et al.*, "Economic overview of the use and production of photovoltaic solar energy in brazil," *Renew. Sustain. Energy Rev.*, vol. 81, no. April 2016, pp. 181–191, 2018.

[21] MESSAOUDA AZZOUZI & MILAN STORK, "Modeling and Simulation of a Photovoltaic Cell Considering Single-Diode Model," *MPACT Int. J. Res. Eng. Technol. (IMPACT IJRET)*, vol. 2, no. 11, pp. 19–28, 2014.

[22] C. A. F. Fernandes, J. P. N. Torres, P. J. C. Branco, J. Fernandes, and J. Gomes, "Cell string layout in solar photovoltaic collectors," *Energy Convers. Manag.*, 2017.

[23] S. Bhattacharjee and B. J. Saharia, "A comparative study on converter topologies for maximum power point tracking application in photovoltaic generation," *J. Renew. Sustain. Energy*, vol. 6, no. 5, 2014.

[24] H. Patel, V. Agarwal, and S. Member, "MATLAB-based modeling .pdf," vol. 23, no. 1, pp. 302–310, 2008.

[25] S. M. Sze and G. Gibbons, "Effect of junction curvature on breakdown voltage in semiconductors," *Solid. State. Electron.*, vol. 9, no. 9, pp. 831–845, Sep. 1966.

[26] S. Iwata, S. Shibakawa, N. Imawaka, and K. Yoshino, "Stability of the current characteristics of dye-sensitized solar cells in the second quadrant of the current–voltage characteristics," *Energy Reports*, vol. 4, pp. 8–12, Nov. 2018.

[27] V. Quaschning and R. Hanitsch, "Numerical simulation of photovoltaic generators with shaded cells," *30th Univ. Power Eng. Conf. Greenwich*, pp. 583–586, 1995.

[28] B. B. Pannebakker, A. C. De Waal, and W. G. J. H. M. Van Sark, "Photovoltaics in the shade: one bypass diode per solar cell revisited," 2017.

[29] S. Harb, M. Kedia, H. Zhang, and R. S. Balog, "Microinverter and string inverter grid-connected photovoltaic system — A comprehensive study," in *2013 IEEE 39th Photovoltaic Specialists Conference (PVSC)*, 2013, pp. 2885–2890.

[30] D. K. Perovich, "Light reflection and transmission by a temperate snow cover," *J. Glaciol.*, vol. 53, no. 181, pp. 201–210, 2007.

[31] J. A. Duffie and W. A. Beckman, *Solar Radition*, vol. 116. 2003.

[32] C. Deline, J. Meydbray, M. Donovan, and J. Forrest, "Photovoltaic shading testbed for module-level power electronics," *Contract*, vol. 303, no. May, pp. 275–3000, 2012.

[33] S. G. Warren, "Optical properties of snow," *Rev. Geophys.*, vol. 20, no. 1, p. 67, 1982.

[34] P. I. Cooper, "The absorption of radiation in solar stills," *Sol. Energy*, vol. 12, no. 3, pp. 333–346, Jan. 1969.

Appendix A

- **Tree height calculations**

The length of the tree is calculated to project shade on the middle of the two PV systems at least up to the upper row by the 17th of May. This gives the day number $n = 137$

The declination angle (δ) can be thus obtained from the approximate equation of Cooper [34]:

$$\delta = 23.45 \sin\left(360 \frac{284 + n}{365}\right) = 19.26° \quad (1)$$

The coordinates of the systems are the following:

Latitude (ϕ): 60.56, Longitude (L_{loc}): 17.44

To project the same shade on both systems, the tree is set up in the middle so that the shade is perpendicular to them at solar noon. Neglecting the minute correction, the hour angle (ω) is zero at solar noon.

Known this, the solar zenith angle (θ_z) and the solar altitude (α_s) are:

$$\cos(\theta_z) = \cos(\phi)\cos(\delta)\cos(\omega) + \sin(\phi)\sin(\delta) \rightarrow \theta_z = 41.3° \quad (2)$$

$$\alpha_s = (90° - \theta_z) = 48.7° \quad (3)$$

Basic geometry is henceforth used to calculate the height of the tree with this angle. The horizontal distance from tree to the bottom row of the modules is 4.93 m. The systems are installed at 2.55 m height from the level the bottom of tree is set. The two rows of solar panels have a total length of 3.30 m, and since they are tilted 20 degrees, the height from the bottom to the upper row is 1.13 m, and their horizontal projection is 3.10 m. The total horizontal length from the top of the modules to the tree is 8.03 m. The vertical distance from the top of the systems to the top of the tree is obtained from the relation of α_s and the total horizontal distance D=8.03 m:

$$\sin(\alpha_s) = H/D \quad (4)$$

This gives the value H=6.03 m

Therefore, the total vertical height of the tree is

$$H_{tree} = H + 1.13 + 2.55 = 9.7\ m \quad (5)$$

This is the total length of the tree to shade both rows of modules at the 17th of May at solar noon.

- **Solar noon calculation**

Solar time does not always coincide with the local time. In order to know the exact time that solar noon occurs, the standard time must be corrected. The solar noon for the time of the year the experiments are conducted, which is April and May, is forward shifted one hour due to daylight saving time, meaning that in reality it happens at 13:00 instead of 12:00 hours. This corresponds to the local standard clock time term of the following equation:

$$Solar\ Time = Standard\ Time + 4(L_{st} - L_{loc}) + E \quad (6)$$

Where Lst is the standard meridian for the local time zone, L_{loc} is the longitude of the location in question, which are given in degrees west ($0° < L_{loc} < 360°$). These values are L_{loc}: 17.44° and L_{st}: -15°. The parameter E is the minute correction as a function of the time of the year, which is calculated with Equation 7:

$$E = 229.2(0.000075 + 0.001868\ cosB\ - 0.032077\ sinB \quad (7)$$
$$- 0.014615\ cos\ 2B\ - 0.04089\ sin\ 2B = 3.91\ min$$

Where B (rad) is calculated from Equation 8, where n is the day number ($1 \leq n \leq 365$):

$$B\ =\ n - 136/365 = 134.14° = 2.34\ rad \quad (8)$$

Note that the equation of time E has a nonlinear dependency with time as it can be seen in Fig. 1:

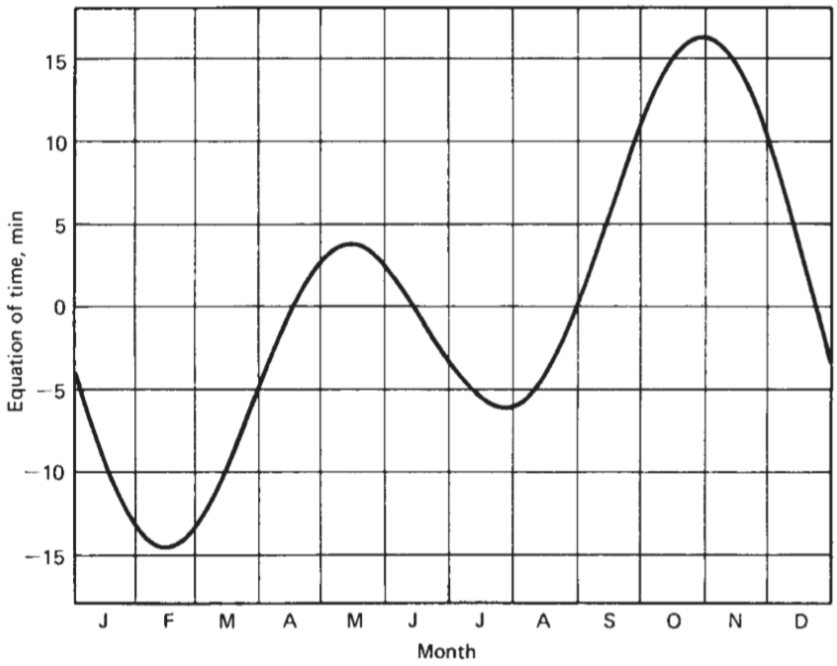

Fig. 1: Equation of time E [31]

Being the Standard Time for solar noon 13:00, the Equation 6 gives the Solar Time, which is at 12:47 hours.

- **Fabric mesh transmittance**

To calculate the transmittance of the cloth used for the experiments, which is the amount of sunlight that passes through it and reaches the solar panels, the normalized production of the solar panels for unshaded conditions is compared to their production under the fabric mesh. This comparison is valid because both scenarios have similar irradiance. The transmittance of each system can be seen from Fig. 2, and it is calculated as follows:

$$Transmittance = \frac{Normalized\ prod.under\ fabric\ mesh}{Normalized\ prod.unshaded\ conditions} \quad (9)$$

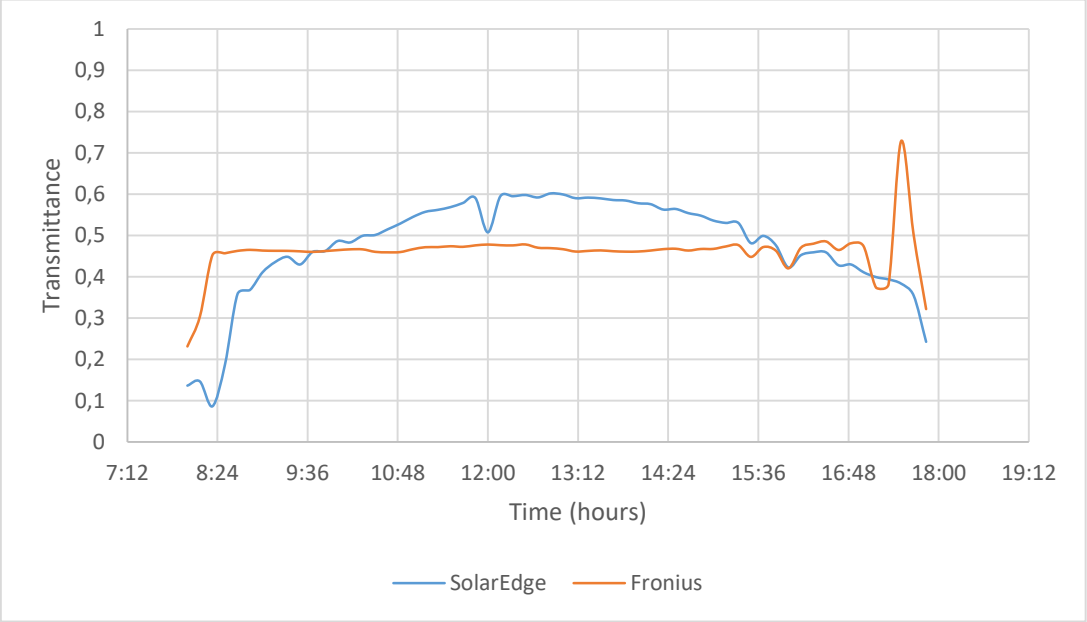

Fig. 2: Transmittance of the fabric mesh for both systems during the day

- **System efficiency calculation**

The efficiency of the systems is calculated with the production data (W/m^2) and the irradiance received (W/m^2) during the daytime, as it is seen in Equation 11:

$$\eta = \frac{Total\ system\ production\ (W)/Total\ system\ front\ Area\ (m^2)}{Irradiance\ (W/m^2)} \tag{10}$$

Where the total area of the system is calculated with the area of the solar cells comprising the modules and the number of modules:

$$Total\ system\ front\ Area\ (m^2) = Cell\ Area\ (m^2) \cdot N\frac{cells}{module} \cdot N\frac{modules}{system} \tag{11}$$

All these values are found in the datasheets in Appendix D.

The data regarding the irradiance and the system production is obtained with the reference solar cell and the power meter PQube, respectively. Fig. 3 shows the efficiency of both systems during a one-day time period.

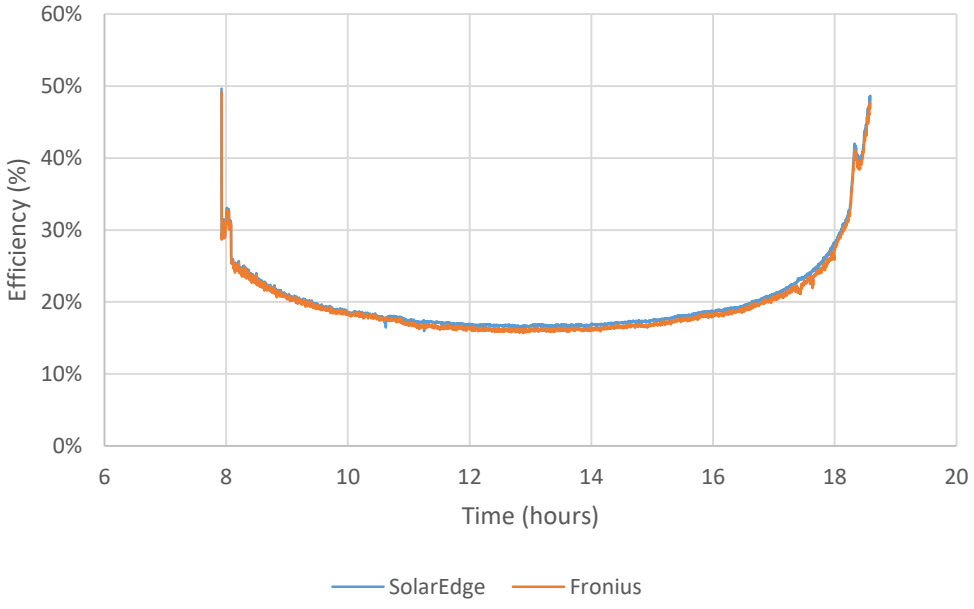

Fig. 3: Efficiency of SolarEdge and Fronius systems

Appendix B

Table 1: PV module and test parameters for I-V measurements with Eurolink PRO instrument

PV System		SolarEdge
Solar panel manufacturer		JinkoSolar
Module type		JKM270PP-60
Electrical Parameters (STC)		
Maximum Power	Pmax	260 W peak
Maximum Power Voltage	Vmpp	31.7 V
Maximum Power Current	Impp	8.52 A
Open Circuit Voltage	Voc	38.8 V
Short Circuit Current	Isc	9.09 A
Thermal Characteristics		
Nominal Operating Cell Temperature	NOCT	45 ± 2 °C
Temperature coefficient of Isc	α	0.06 mA/°C
Temperature coefficient of Voc	β	-0.30 V/°C
Temperature coefficient of Pmax	γ	-0.40 %/°C
Measurement parameters		
Testing standard		IEC 60891
Irradiance sensor		PV solar cell
Minimum irradiance		500 W/m²
Operating sensor temperature		Cell temperature
Modules in series		1
Modules in series		1

The serial resistance of the PV module (Rs) is assumed to be 0.4 Ω.

- **I-V characteristic and power graph of JinkoSolar module with EuroLink PRO under shading patterns corresponding to Measurement 0 to 7**

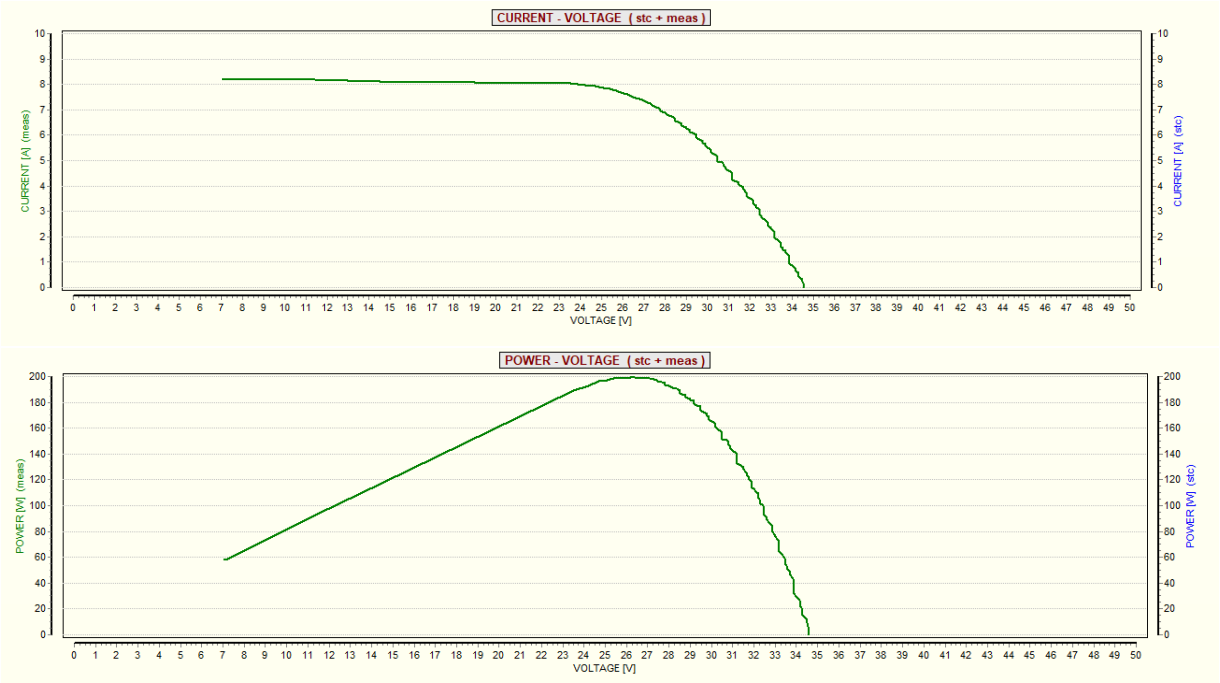

Fig. 1: Measurement 0

Fig. 2: Measurement 1

Fig. 3: Measurement 2

Fig. 4: Measurement 3

Fig. 5: Measurement 4

Fig. 6: Measurement 5

Fig. 7: Measurement 6

Appendix C

Table 1: PV module and test parameters for I-V measurements with Eurolink PRO instrument

PV System		Stand-alone module
Solar panel manufacturer		SolarWorld
Module type		Sunmodule sw 50 poly RMA
Electrical Parameters (STC)		
Maximum Power	Pmax	50 W peak
Maximum Power Voltage	Vmpp	18.2 V
Maximum Power Current	Impp	2.75 A
Open Circuit Voltage	Voc	22.1 V
Short Circuit Current	Isc	2.95 A
Thermal Characteristics		
Nominal Operating Cell Temperature	NOCT	46 °C
Temperature coefficient of Isc	α	0.034 mA/°C
Temperature coefficient of Voc	β	-0.34 V/°C
Temperature coefficient of Pmax	γ	-0.48 %/°C
Measurement parameters		
Testing standard		IEC 60891
Irradiance sensor		PV solar cell
Minimum irradiance		500 W/m^2
Operating sensor temperature		Cell temperature
Modules in series		1
Modules in series		1

The serial resistance of the PV module (Rs) is assumed to be 0.4 Ω.

- **I-V characteristic and power graph of SunModule sw50 with EuroLink PRO under shading patterns corresponding to Cases 0 to 12**

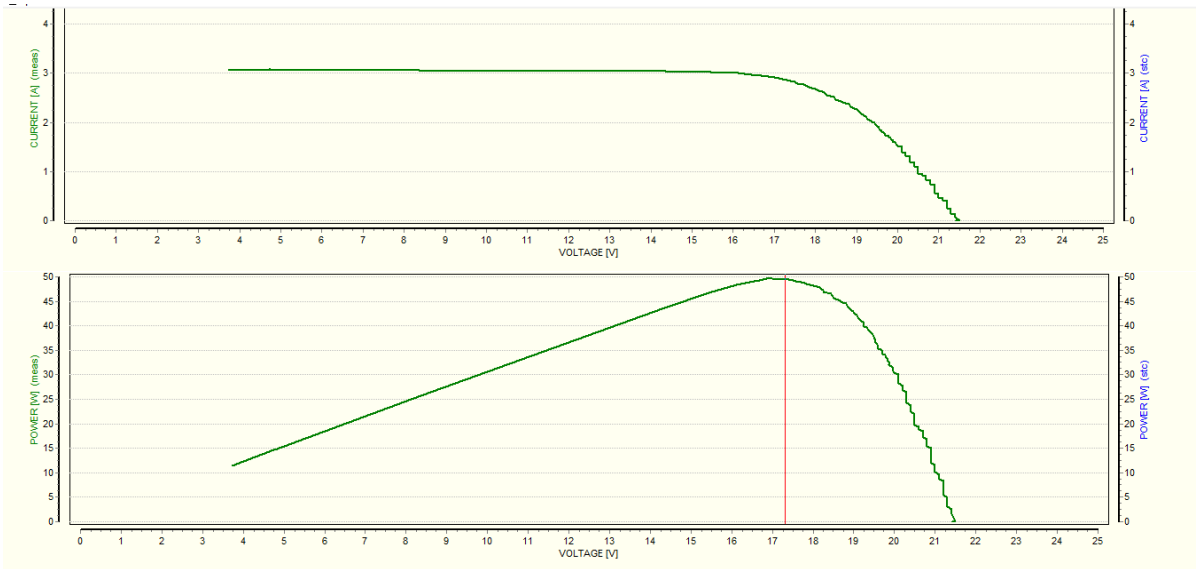

Fig. 1: Case 0

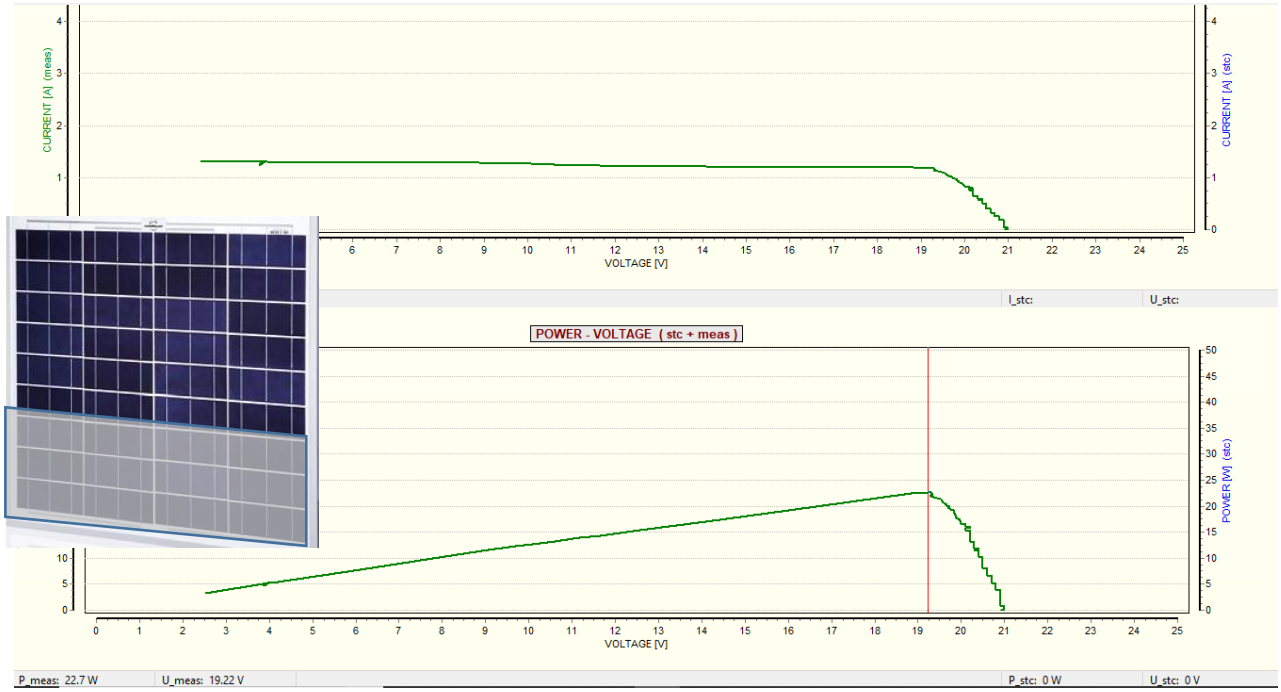

Fig. 2: Case 1

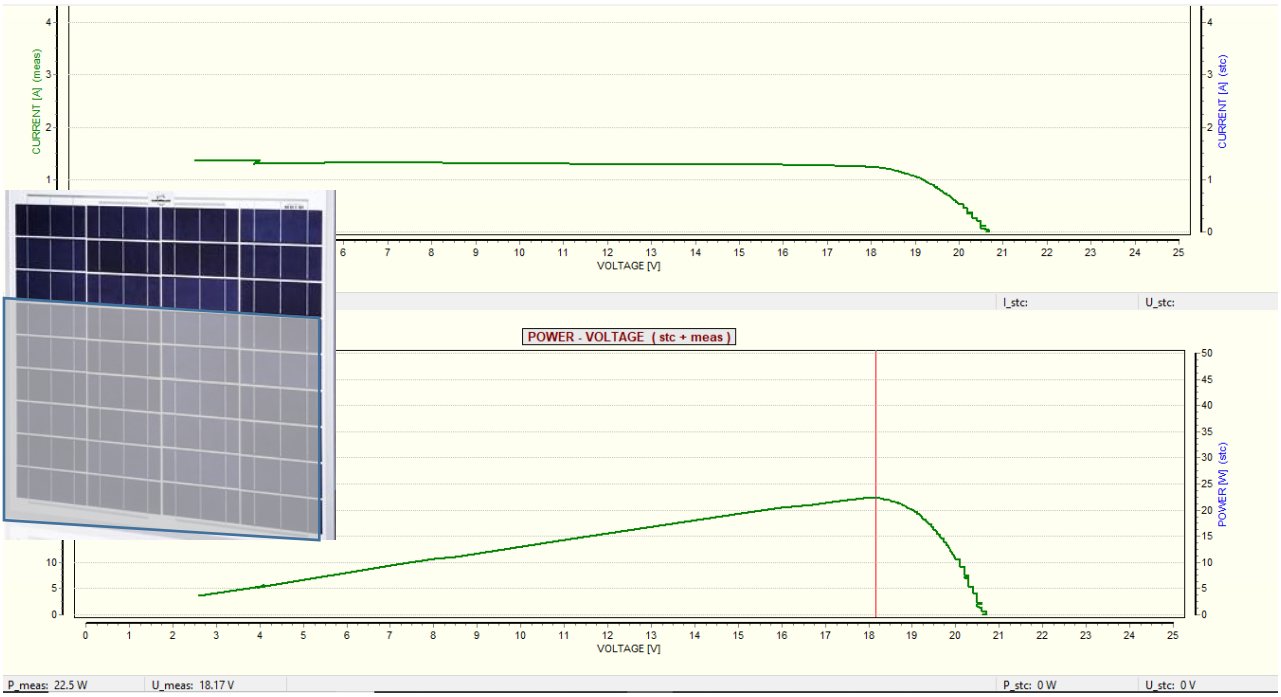

Fig. 3: Case 2

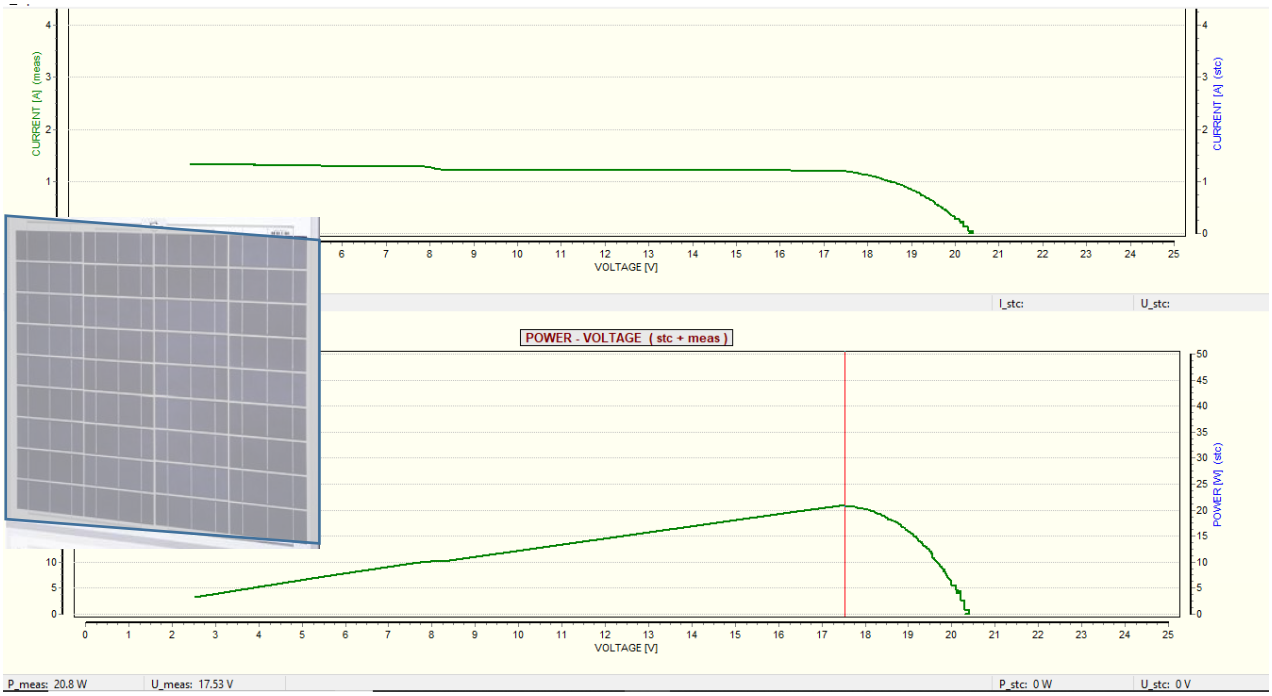

Fig. 4: Case 3

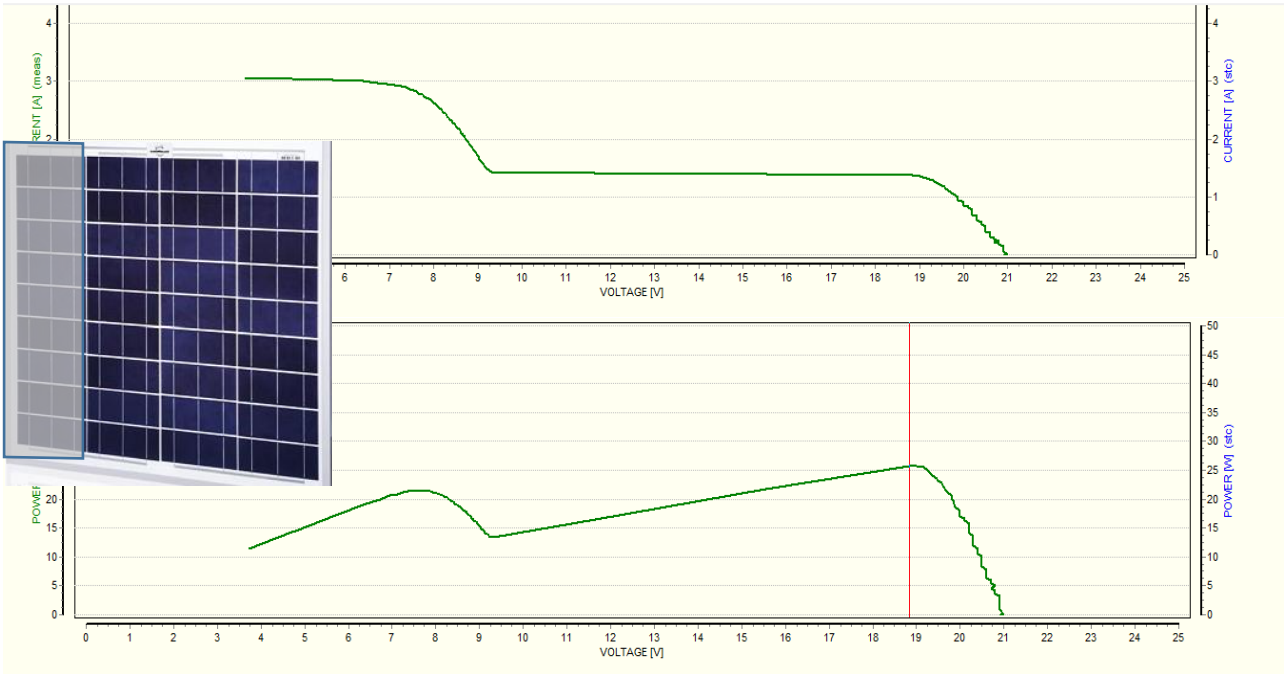

Fig. 5: Case 4

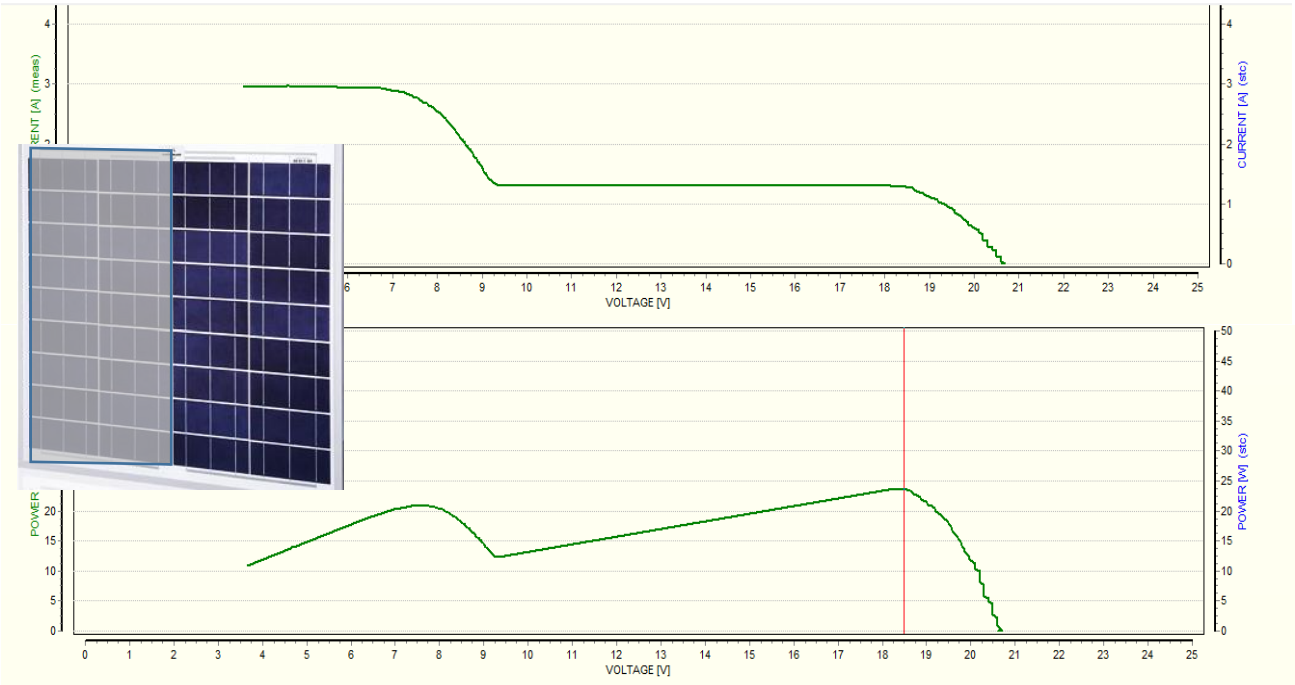

Fig. 6: Case 5

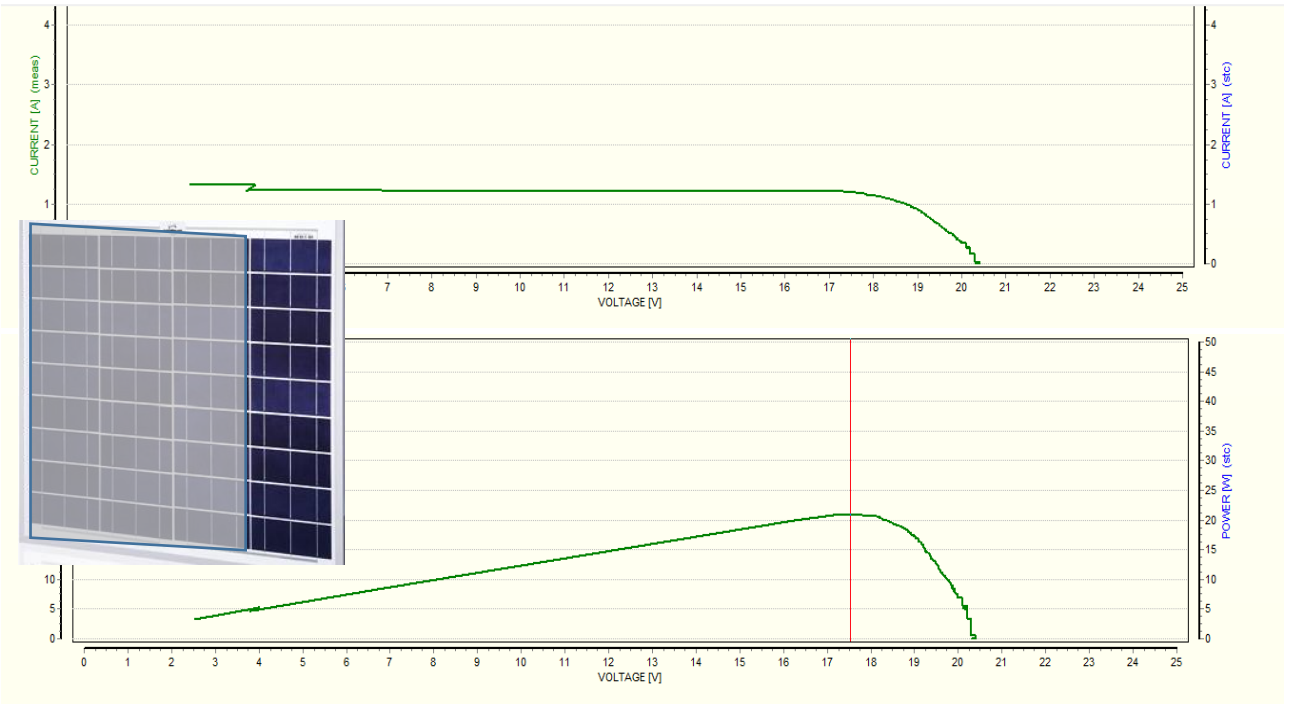

Fig. 7: case 6

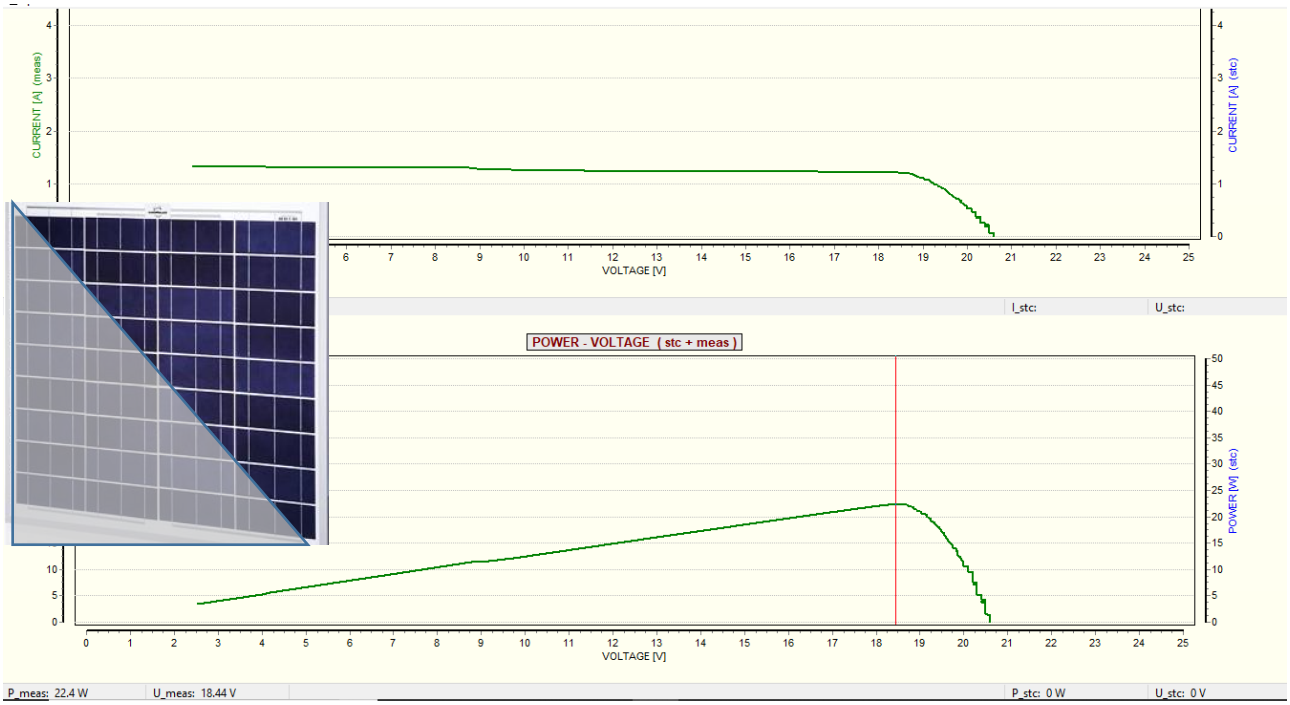

Fig. 8: Case 7

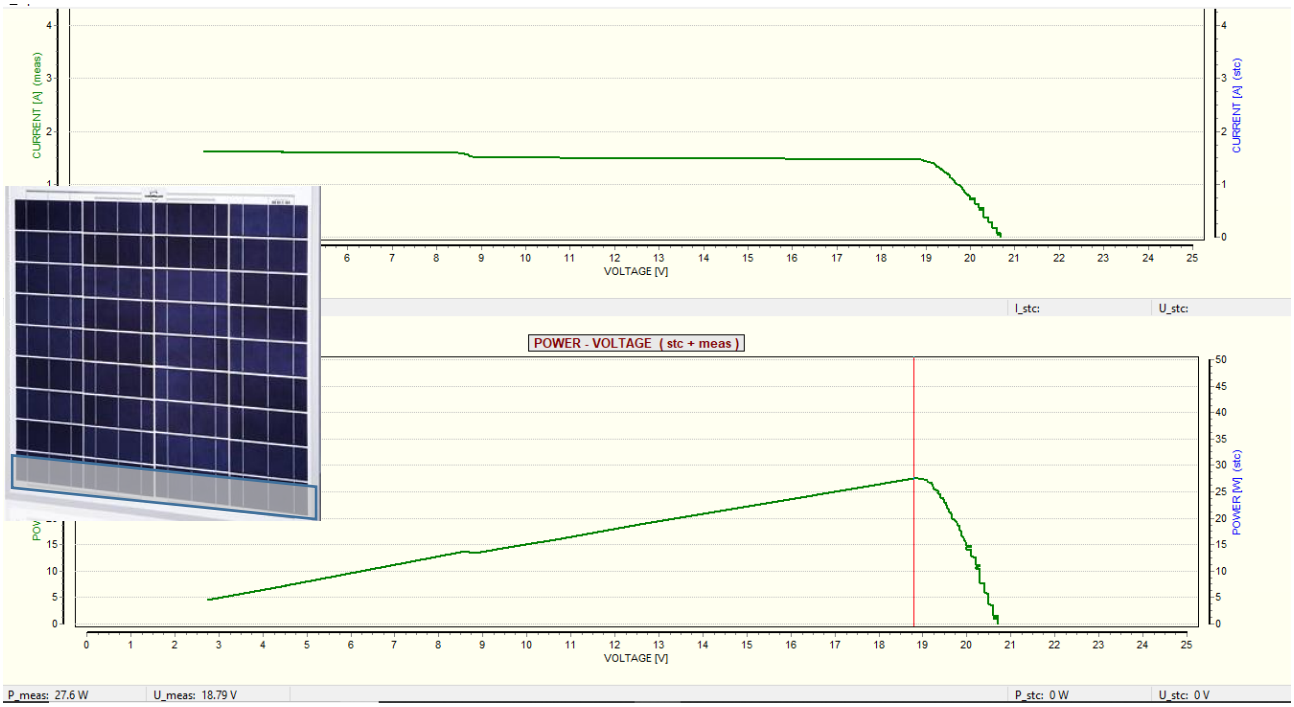

Fig. 9: Case 8

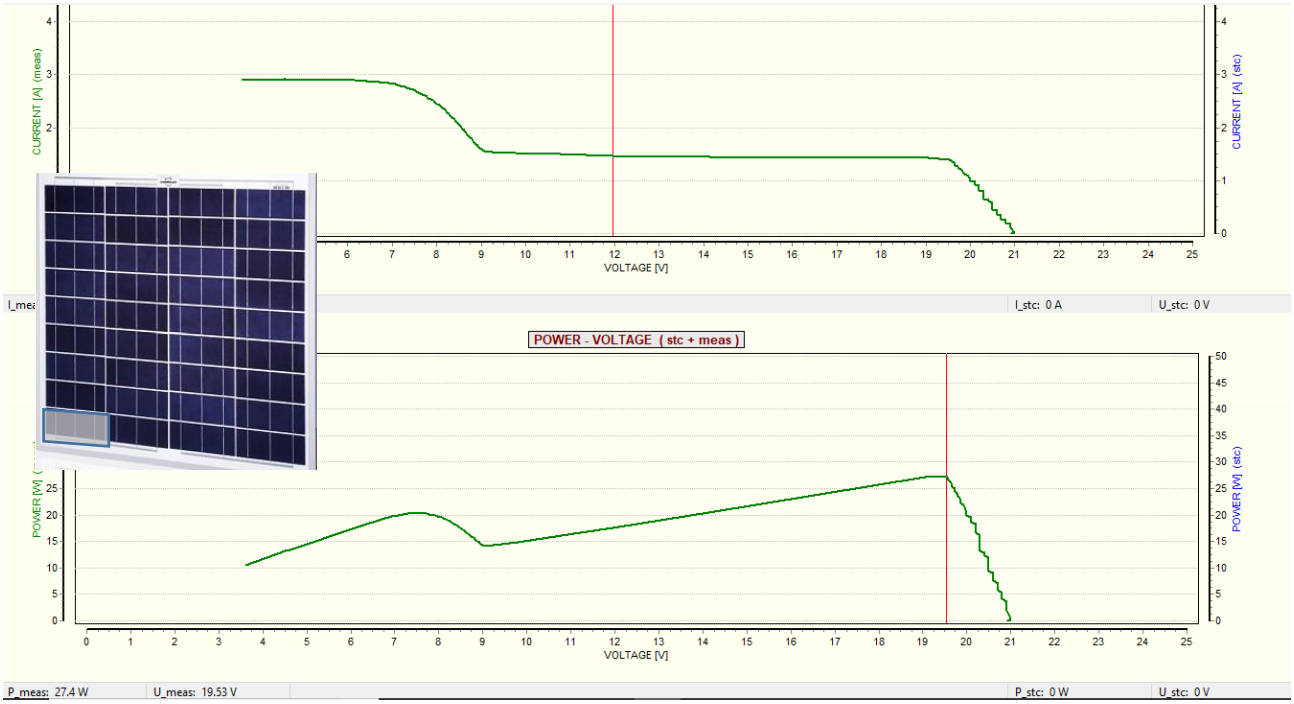

Fig. 10: Case 9

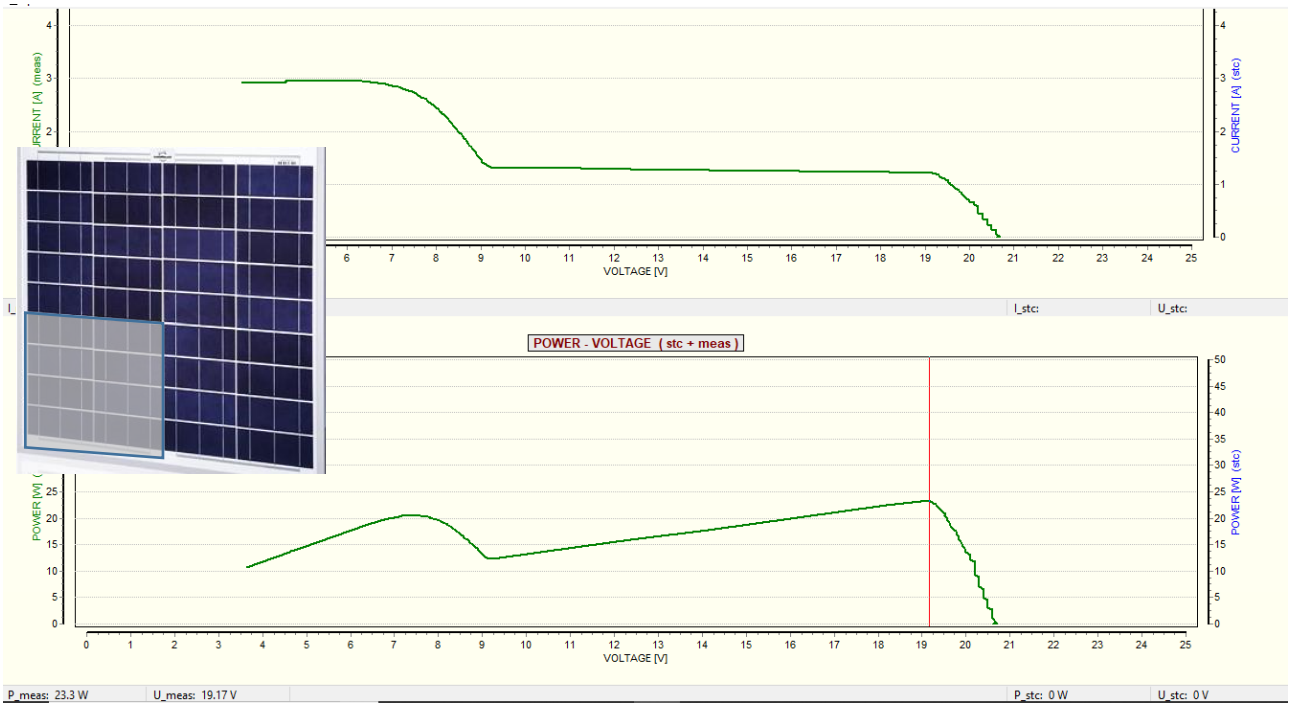

Fig. 11: Case 10

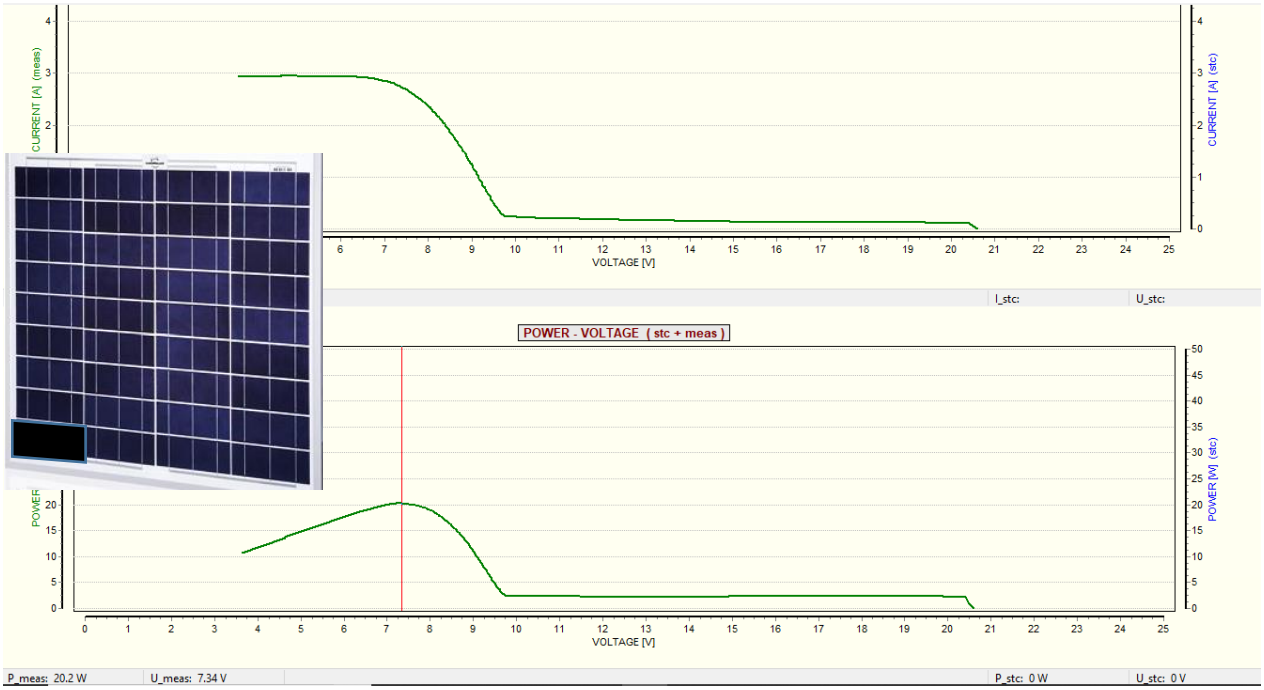

Fig. 12: Case 11

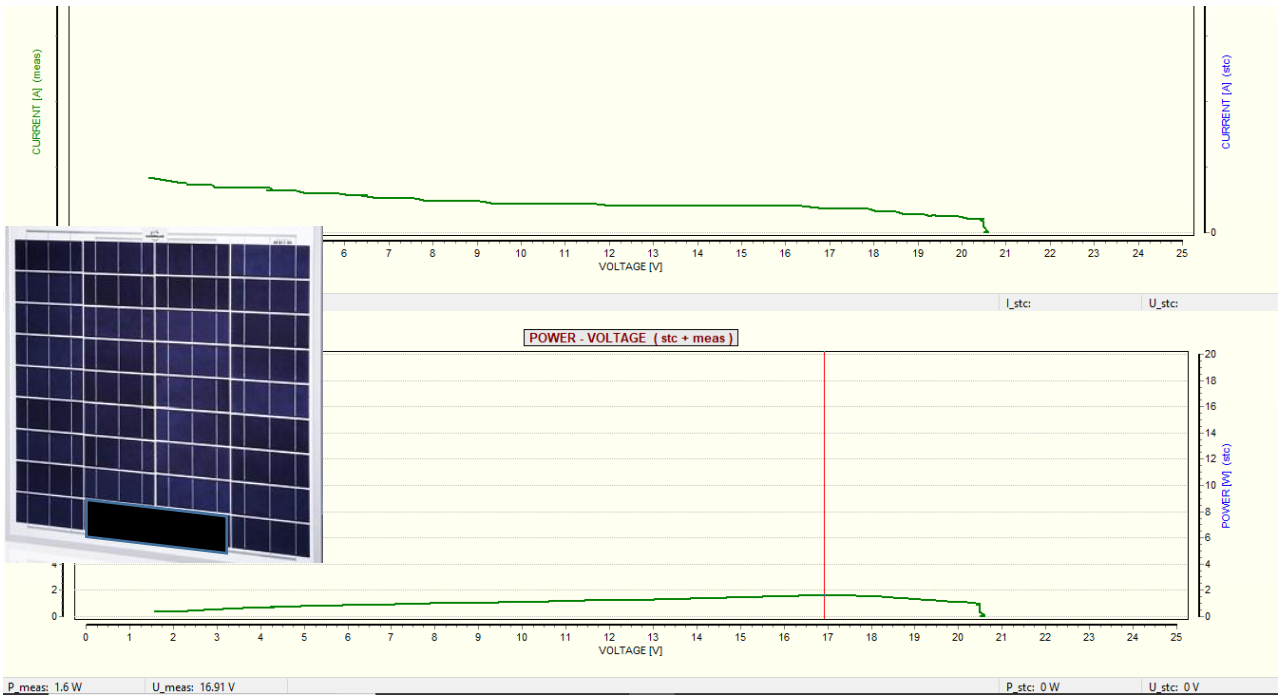

Fig. 13: Case 12

Appendix D

Table 1: Technical specifications of SolarEdge and Fronius systems

PV System		SolarEdge		Fronius	
Solar panel manufacturer		JinkoSolar		YingliSolar	
Module type		JKM270PP-60		YL275C-30b	
Electrical Parameters					
		STC	NOCT	STC	NOCT
Maximum Power	Pmax	260 Wp	202 Wp	275 Wp	198.6 Wp
Power tolerance	ΔPmax	0 ~ +3%		0 ~ +0.02 %	
Maximum Power Voltage	Vmpp	31.7 V	29.0 V	30.9 V	28.3 V
Maximum Power Current	Impp	8.52 A	6.97 A	8.91 A	7.02 A
Open Circuit Voltage	Voc	38.8 V	35.6 V	38.8 V	36.7 V
Short Circuit Current	Isc	9.09 A	7.35 A	9.47 A	7.23 A
Module Efficiency STC	η	16.5 %		16.8 %	
Thermal Characteristics					
Nominal Operating Cell Temperature	NOCT	45 ± 2 °C		46 ± 2 °C	
Temperature coefficient of Isc	α	0.06 mA/°C		0.04 %/°C	
Temperature coefficient of Voc	β	-0.30 V/°C		-0.31 %/°C	
Temperature coefficient of Pmax	γ	-0.40 %/°C		-0.42 %/°C	
Operating Conditions					
Maximum System Voltage (IEC)		1000 V_{DC}		1000 V_{DC}	
Maximum Series Fuse rating		15 A		20 A	
Operating Temperature range		-40°C ~ +85°C			
Construction Materials					
Cell (Quantity/Type/Dimensions)		60/Poly-crystalline/156×156mm		60/Monocrystalline silicon/156×156 mm	
Front Glass (Material/Thickness)		Low-iron tempered glass, anti-reflection coating, high transmission / 3.2mm		Low-iron tempered glass / 3.2mm	
Dimensions (L×W×H)		1650×992×40mm		1650×990×40mm	
Weight		19.0 kg		19.1kg	
Frame		Anodized aluminum alloy		Anodized aluminum alloy	
Junction Box		IP67 Rated		≥ IP65	
Output Cables (Length/Cross-sectional area		900mm/4mm^2		1100mm/4mm^2	

*STC: Standard Conditions at 1000W/m^2 irradiance, 25°C cell temperature, AM1.5g spectrum according to EN 60904-3

**NOCT: open-circuit module operation Temp. at 800W/m^2 irradiance, 20°C ambient temperature, AM1.5, 1m/s wind speed

www.jinkosolar.com

Solar
JinKO
Building **Your Trust** in Solar

Eagle 60
260-280 Watt

POLY CRYSTALLINE MODULE

Positive power tolerance of 0~+3%

ISO9001:2008、ISO14001:2004、OHSAS18001 certified factory.
IEC61215、IEC61730 certified products.

(4BB)

KEY FEATURES

4 Busbar Solar Cell:

4 busbar solar cell adopts new technology to improve the efficiency of modules , offers a better aesthetic appearance, making it perfect for rooftop installation.

High Power Output:

Polycrystalline 60-cell module achieves a power output up to 280Wp.

PID RESISTANT:

Limited power degradation of Eagle module caused by PID effect is guaranteed under strict testing condition (85℃/85%RH,96hours)for mass production.

Low-light Performance:

Advanced glass and surface texturing allow for excellent performance in low-light environments.

Severe Weather Resilience:

Certified to withstand: wind load (2400 Pascal) and snow load (5400 Pascal).

Durability against extreme environmental conditions:

High salt mist and ammonia resistance certified by TUV NORD.

Temperature Coefficient:

Improved temperature coefficient decreases power loss during high temperatures.

LINEAR PERFORMANCE WARRANTY

10 Year Product Warranty • 25 Year Linear Power Warranty

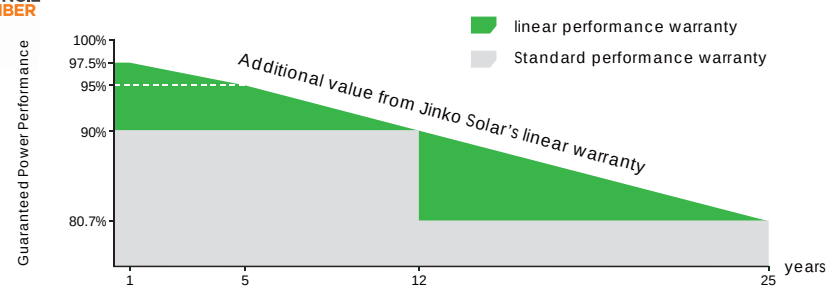

Engineering Drawings

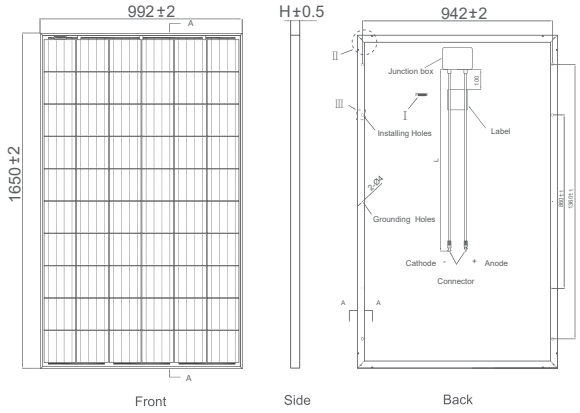

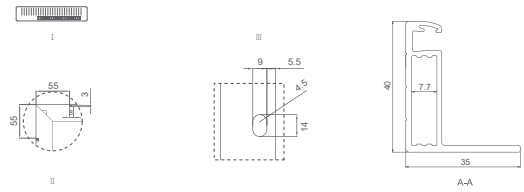

Packaging Configuration

(Two boxes=One pallet)

26pcs/box, 52pcs/pallet, 728 pcs/40'HQ Container

Electrical Performance & Temperature Dependence

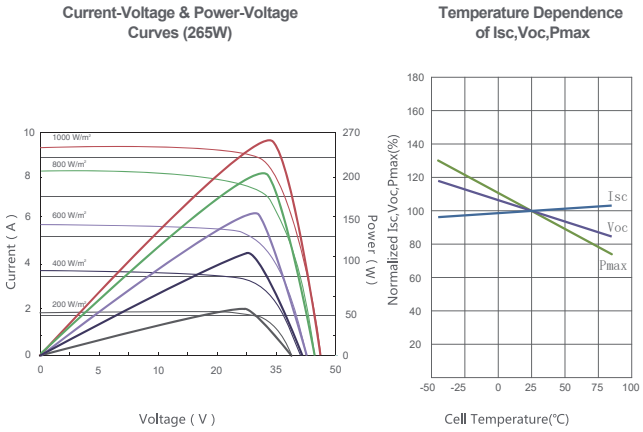

Mechanical Characteristics

Cell Type	Poly-crystalline 156×156mm (6 inch)
No.of cells	60 (6×10)
Dimensions	1650×992×40mm (65.00×39.05×1.57 inch)
Weight	19.0 kg (41.9 lbs)
Front Glass	3.2mm, Anti-Reflection Coating, High Transmission, Low Iron, Tempered Glass
Frame	Anodized Aluminium Alloy
Junction Box	IP67 Rated
Output Cables	TÜV 1×4.0mm², Length: 900mm or Customized Length

SPECIFICATIONS

Module Type	JKM260PP-60		JKM265PP-60		JKM270PP-60		JKM275PP-60		JKM280PP-60	
	STC	NOCT	STC	NOCT	STC	NOCT	STC	NOCT	STC	NOCT
Maximum Power (Pmax)	260Wp	194Wp	265Wp	198Wp	270Wp	202Wp	275Wp	205Wp	280Wp	209Wp
Maximum Power Voltage (Vmp)	31.1V	28.3V	31.4V	28.7V	31.7V	29.0V	32.0V	29.3V	32.3V	29.6V
Maximum Power Current (Imp)	8.37A	6.84A	8.44A	6.91A	8.52A	6.97A	8.61A	7.00A	8.69A	7.06A
Open-circuit Voltage (Voc)	38.1V	35.1V	38.6V	35.3V	38.8V	35.6V	39.1V	35.9V	39.4V	36.1V
Short-circuit Current (Isc)	8.98A	7.26A	9.03A	7.31A	9.09A	7.35A	9.15A	7.37A	9.20A	7.42A
Module Efficiency STC (%)	15.89%		16.19%		16.50%		16.80%		17.11%	
Operating Temperature(℃)	-40℃~+85℃									
Maximum system voltage	1000VDC (IEC)									
Maximum series fuse rating	15A									
Power tolerance	0~+3%									
Temperature coefficients of Pmax	-0.40%/℃									
Temperature coefficients of Voc	-0.30%/℃									
Temperature coefficients of Isc	0.06%/℃									
Nominal operating cell temperature (NOCT)	45±2℃									

*STC: Irradiance 1000W/m² Cell Temperature 25°C AM=1.5

NOCT: Irradiance 800W/m² Ambient Temperature 20°C AM=1.5 Wind Speed 1m/s

* Power measurement tolerance: ± 3%

PANDA 60 Cell
40mm SERIES

YL280C-30b
YL275C-30b
YL270C-30b
YL265C-30b
YL260C-30b
YL255C-30b
YL250C-30b

panda
Powered by YINGLI

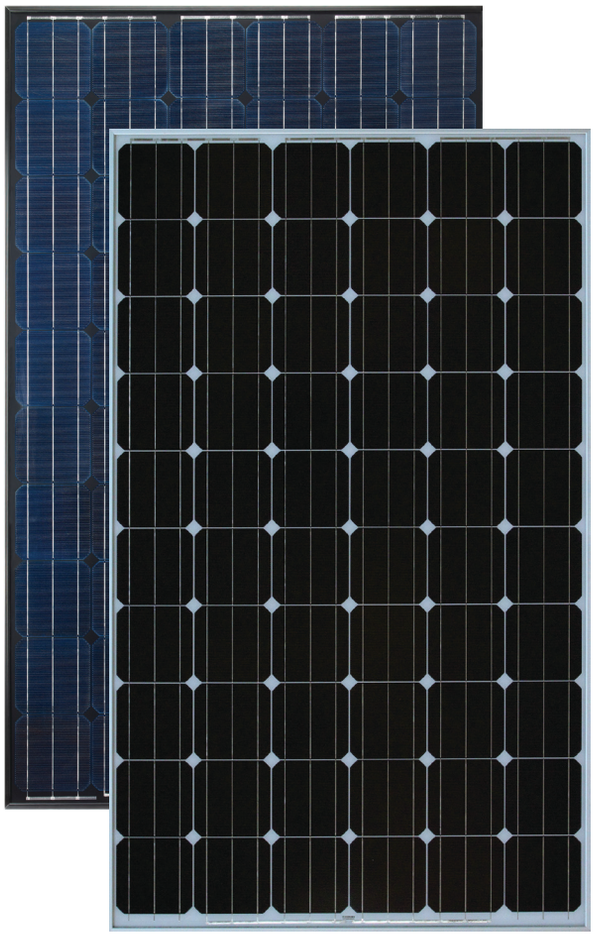

ABOUT YINGLI GREEN ENERGY

Yingli Green Energy Holding Company Limited (NYSE: YGE) is one of the world's largest fully vertically integrated PV manufacturers, which markets its products under the brand "Yingli Solar". With over 4.5GW of modules installed globally, we are a leading solar energy company built upon proven product reliability and sustainable performance. We are the first renewable energy company and the first Chinese company to sponsor the FIFA World Cup™.

PERFORMANCE

- Yingli Solar PANDA is a new monocrystalline silicon module technology with n-type solar cells that have average efficiencies higher than 19.5%. Combined with high transmission glass, module efficiencies are up to 17.1%.
- Compared to traditional modules with p-type solar cells, PANDA modules have lower initial degradation and higher performance under both high temperature and low irradiation conditions.
- Tight positive power tolerance of 0W to +5W ensures you receive modules at or above nameplate power and contributes to minimizing module mismatch losses leading to improved system yield.
- Top ranking in the "TÜV Rheinland Energy Yield Test" demonstrates high performance and annual energy production.

RELIABILITY

- Tests by independent laboratories prove that Yingli Solar modules:
  - ✓ Fully conform with certification and regulatory standards.
  - ✓ Withstand wind loads of up to 2.4kPa and snow loads of up to 5.4kPa, confirming mechanical stability.
  - ✓ Successfully endure ammonia and salt-mist exposure at the highest severity level, ensuring their performance in adverse conditions.
- Manufacturing facility certified by TÜV Rheinland to ISO 9001:2008, ISO 14001:2004 and BS OHSAS 18001:2007.

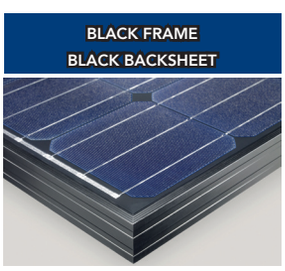

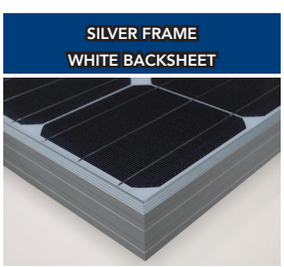

WARRANTIES

- 10-year limited product warranty[1].
- Limited power warranty[1]: 1 year at 98% of the minimal rated power output, 10 years at 92% of the minimal rated power output, 25 years at 82% of the minimal rated power output.

[1]In compliance with our Warranty Terms and Conditions.

QUALIFICATIONS & CERTIFICATES

IEC 61215, IEC 61730, MCS, CE, ISO 9001:2008, ISO 14001:2004, BS OHSAS 18001:2007, SA 8000, PV Cycle

YINGLISOLAR.COM

PANDA 60 Cell 40mm SERIES

ELECTRICAL PERFORMANCE

Electrical parameters at Standard Test Conditions (STC)

Module type			YLxxxC-30b (xxx=P_{max})						
Power output	P_{max}	W	280	275	270	265	260	255	250
Power output tolerances	ΔP_{max}	W	0 / 5						
Module efficiency	η_m	%	17.1	16.8	16.5	16.2	15.9	15.6	15.3
Voltage at P_{max}	V_{mpp}	V	31.1	30.8	31.1	31.0	30.8	30.6	30.5
Current at P_{max}	I_{mpp}	A	9.01	8.94	8.68	8.55	8.46	8.33	8.20
Open-circuit voltage	V_{oc}	V	38.9	38.6	39.0	39.0	38.6	38.3	38.1
Short-circuit current	I_{sc}	A	9.61	9.55	9.06	8.93	8.91	8.85	8.71

STC: 1000W/m² irradiance, 25°C cell temperature, AM1.5g spectrum according to EN 60904-3.
Average relative efficiency reduction of 3.5% at 200W/m² according to EN 60904-1.

Electrical parameters at Nominal Operating Cell Temperature (NOCT)

Power output	P_{max}	W	202.2	198.6	194.7	192.4	188.8	185.2	181.6
Voltage at P_{max}	V_{mpp}	V	28.3	28.3	28.2	28.1	27.8	27.7	27.6
Current at P_{max}	I_{mpp}	A	7.14	7.02	6.91	6.86	6.79	6.68	6.58
Open-circuit voltage	V_{oc}	V	37.1	36.7	36.2	35.9	35.5	35.2	35.1
Short-circuit current	I_{sc}	A	7.27	7.23	7.21	7.20	7.18	7.13	7.02

NOCT: open-circuit module operation temperature at 800W/m² irradiance, 20°C ambient temperature, 1m/s wind speed.

THERMAL CHARACTERISTICS

Nominal operating cell temperature	NOCT	°C	46 +/- 2
Temperature coefficient of P_{max}	γ	%/°C	-0.42
Temperature coefficient of V_{oc}	β_{Voc}	%/°C	-0.31
Temperature coefficient of I_{sc}	α_{Isc}	%/°C	0.04
Temperature coefficient of V_{mpp}	β_{Vmpp}	%/°C	-0.41

OPERATING CONDITIONS

Max. system voltage	1000V_{DC}
Max. series fuse rating	20A
Limiting reverse current	20A
Operating temperature range	-40°C to 85°C
Max. static load, front (e.g., snow and wind)	5400Pa
Max. static load, back (e.g., wind)	2400Pa
Max. hailstone impact (diameter / velocity)	25mm / 23m/s

CONSTRUCTION MATERIALS

Front cover (material / thickness)	low-iron tempered glass / 3.2mm
Backsheet (color)	white or black
Cell (quantity / material / dimensions)	60 / monocrystalline silicon / 156mm x 156mm
Encapsulant (material)	ethylene vinyl acetate (EVA)
Frame (material / color / anodization color)	anodized aluminum alloy / silver or black / clear
Junction box (protection degree)	≥ IP65
Cable (length / cross-sectional area)	1100mm / 4mm²
Plug connector (type / protection degree)	MC4 / IP67 or YT08-1 / IP67 or Amphenol H4 / IP68

- Due to continuous innovation, research and product improvement, the specifications in this product information sheet are subject to change without prior notice. The specifications may deviate slightly and are not guaranteed.
- The data do not refer to a single module and they are not part of the offer, they only serve for comparison to different module types.

GENERAL CHARACTERISTICS

Dimensions (L / W / H)	1650mm / 990mm / 40mm
Weight	19.1kg

PACKAGING SPECIFICATIONS

Number of modules per pallet	26
Number of pallets per 40' container	28
Packaging box dimensions (L / W / H)	1700mm / 1150mm / 1190mm
Box weight	534kg

Unit: mm

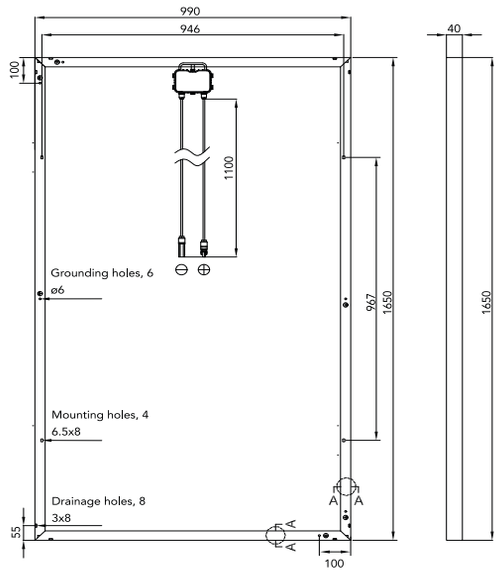

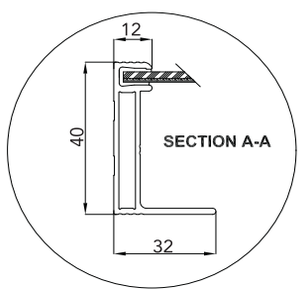

Warning: Read the Installation and User Manual in its entirety before handling, installing, and operating Yingli Solar modules.

Our Partners:

Yingli Green Energy Holding Co. Ltd.
service@yinglisolar.com
Tel: 0086-312-8929802

YINGLISOLAR.COM

YINGLI SOLAR OFFICIAL SPONSOR FIFA WORLD CUP Brasil 2014

Length	26.77 in (680 mm)
Width	26.77 in (680 mm)
Height	1.34 in (34 mm)
Frame	Aluminum
Weight	5.6 kg

ÖKO-TEST
LIFE WORTH LIVING
SolarWorld
Sunmodule Plus
SW 225 poly
excellent
issue 05/2010

Sunmodule®
SW 50 poly RMA

World class quality
SolarWorld produces the best products with the highest quality, manufactured according to German and US quality standards in fully-automated ISO 9001 and 14001 certified factories.

Outstanding products
SolarWorld's modules were assessed by the ÖKO-TEST consumer magazine as "excellent".

An experienced industry leader
With over 30 years of experience in off-grid solar applications – SolarWorld delivers top products and technical experience at the highest levels. Our modules are installed in over 100,000 Telecom/Industrial systems worldwide. Nobody else comes close.

SOLARWORLD

We turn sunlight into power.

www.solarworld-usa.com

Sunmodule®
SW 50 poly RMA

PERFORMANCE UNDER STANDARD TEST CONDITIONS (STC)*

		SW 50
Maximum power	P_{max}	50 Wp
Open circuit voltage	U_{oc}	22.1 V
Maximum power point voltage	U_{mpp}	18.2 V
Short circuit current	I_{sc}	2.95 A
Maximum power point current	I_{mpp}	2.75 A

*STC: 1000W/m², 25°C, AM 1.5

PERFORMANCE AT 800 W/m², NOCT, AM 1.5

		SW 50
Maximum power	P_{max}	35.9 Wp
Open circuit voltage	U_{oc}	19.8 V
Maximum power point voltage	U_{mpp}	16.3 V
Short circuit current	I_{sc}	2.38 A
Maximum power point current	I_{mpp}	2.20 A

Minor reduction in efficiency under partial load conditions at 25°C: at 200W/m², 95% (+/-3%) of the STC efficiency (1000 W/m²) is achieved.

COMPONENT MATERIALS

Cells per module	36
Cell type	Poly crystalline
Cell dimensions	2.44 in x 6.14 in (62 mm x 156 mm)
Front	tempered glass (EN 12150)

SYSTEM INTEGRATION PARAMETERS

Maximum system voltage SC II	1000 V
Maximum reverse current	12 A
Increased snowload acc. to IEC 61215	5.4 kN/m²
Number of bypass diodes	2

THERMAL CHARACTERISTICS

NOCT	46 °C
TC I_{sc}	0.034 %/K
TC U_{oc}	-0.34 %/K
TC P_{mpp}	-0.48 %/K

ADDITIONAL DATA

Power tolerance	+/- 10 %
Junction box	IP65
Maximum outer cable diameter	0.31 in (7.8 mm)
Maximum wire cross section	4 mm²

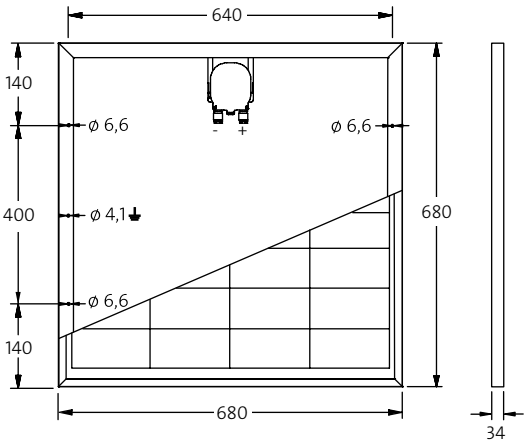

· Qualified, IEC 61215
· Safety tested, IEC 61730
· Periodic Inspection

SolarWorld AG reserves the right to make specification changes without notice. This data sheet complies with the requirements of EN 50380.